

ELECTRON CORRELATION: QUANTUM CHEMISTRY'S HOLY GRAIL

in "NATO-ASI Series in Metal-Ligand Interaction in Molecular-, Nano-, Micro, and Macro-systems in Complex Environments", Ed.: N. Russo, D. R. Salahub and M. Witko, Kluwer Academic Publishers, Dordrecht (2003)

J. M. MERCERO, E. VALDERRAMA AND J. M. UGALDE
Kimika Fakultatea; Euskal Herriko Unibertsitatea
P. K. 1072; 20080 Donostia; Euskadi (Spain)

1. Introduction

The land-mark paper of Heitler and London[1] on the ground state of H_2 opened the way to a theoretical understanding of the chemical bond and marks the birth of quantum chemistry. Interestingly, their trial wave function for the ground state of H_2 includes only *covalent* configurations, *i.e.*, by excluding explicitly *ionic* configurations. Namely, being $\psi_X(\mathbf{r})$ the orbital centered on nucleus X , the Heitler and London ansatz is,

$$\Psi_{HL}(\mathbf{x}_1, \mathbf{x}_2) = \frac{1}{\sqrt{2}} [\psi_A(\mathbf{r}_1)\psi_B(\mathbf{r}_2) + \psi_A(\mathbf{r}_2)\psi_B(\mathbf{r}_1)] \Theta(s_1, s_2) \quad (1)$$

where $\mathbf{x} = (\mathbf{r}, s)$ is the composite spatial plus spin coordinate of the electrons and $\Theta(s_1, s_2)$ is the normalized singlet spin wave function,

$$\Theta(s_1, s_2) = \frac{1}{\sqrt{2}} [\alpha(s_1)\beta(s_2) - \alpha(s_2)\beta(s_1)] \quad (2)$$

Thus the two electrons stay completely out from each other's way.

Shortly after the publication of Heitler and London's paper, Hartree[2], Fock[3] and Slater[4] set the foundations of an alternative view for the solution of interacting electrons. The so-called *Independent Particle Model* (IPM) was based on the concept of the self-consistent field, as the *average* field that each of the electrons experience when the interactions with all the remaining electrons have been averaged over their positions. Within this model, the ground state wave function of H_2 is

$$\begin{aligned} \Psi_{HF}(\mathbf{x}_1, \mathbf{x}_2) &= \frac{1}{2} [\psi_A(\mathbf{r}_1)\psi_B(\mathbf{r}_2) + \psi_A(\mathbf{r}_2)\psi_B(\mathbf{r}_1) \\ &+ \psi_A(\mathbf{r}_1)\psi_A(\mathbf{r}_2) + \psi_B(\mathbf{r}_1)\psi_B(\mathbf{r}_2)] \Theta(s_1, s_2) \end{aligned} \quad (3)$$

where the ionic configurations $\psi_A(\mathbf{r}_1)\psi_A(\mathbf{r}_2)$ and $\psi_B(\mathbf{r}_1)\psi_B(\mathbf{r}_2)$ enter in the wave function with the same weight as the covalent configurations.

Recall that Eq. (3) can be cast as

$$\begin{aligned}\Psi_{HF}(1,2) &= \begin{vmatrix} [\psi_A(1) + \psi_B(1)]\alpha(1) & [\psi_A(1) + \psi_B(1)]\beta(1) \\ [\psi_A(2) + \psi_B(2)]\alpha(2) & [\psi_A(2) + \psi_B(2)]\beta(2) \end{vmatrix} \\ &= \begin{vmatrix} \sigma_g(1) & \bar{\sigma}_g(1) \\ \sigma_g(2) & \bar{\sigma}_g(2) \end{vmatrix}\end{aligned}\quad (4)$$

which constitutes a single determinant constructed with the molecular spin-orbitals $\sigma_g(1) = [\psi_A(1) + \psi_B(1)]\alpha(1)$ and $\bar{\sigma}_g(1) = [\psi_A(1) + \psi_B(1)]\beta(1)$, expressed as a linear combination of the atomic orbitals.

Observe that Eq. (1) cannot be cast as a single determinant. However, clearly Eq. (1) can be cast as a linear combination of the determinant of Eq. (4) and a second determinant constructed with the molecular spin-orbitals $\sigma_u(1) = [\psi_A(1) - \psi_B(1)]\alpha(1)$ and $\bar{\sigma}_u(1) = [\psi_A(1) - \psi_B(1)]\beta(1)$. Namely,

$$\Psi_{HL}(1,2) = \begin{vmatrix} \sigma_g(1) & \bar{\sigma}_g(1) \\ \sigma_g(2) & \bar{\sigma}_g(2) \end{vmatrix} + c \begin{vmatrix} \sigma_u(1) & \bar{\sigma}_u(1) \\ \sigma_u(2) & \bar{\sigma}_u(2) \end{vmatrix}\quad (5)$$

with $c = -1$.

Equations (1) and (5) constitute the exact solution for stretched H_2 . A little algebra yields the exact energy of two infinitely distant hydrogen atoms, as

$$E_{H_2} = 2E_H = \langle \Psi_{HL} | \hat{H} | \Psi_{HL} \rangle\quad (6)$$

where \hat{H} is the Hamiltonian operator of H_2 for $R = |R_A - R_B| \rightarrow \infty$ and E_H is the ground state energy of the hydrogen atom as calculated with the orbital ψ .

However, if we use the ansatz of Eq. (5) to describe the electronic structure of the H_2 at its equilibrium bond length, $R=1.401$ a.u., the result is rather discouraging in spite of the expectations raised by its exactness for $R \rightarrow \infty$. Indeed, for a simple representation of the orbital ψ as a minimum STO-3G basis set[5], we obtain

$$E_{H_2} = -1.1372779 \text{ a.u. and } c = -0.1134\quad (7)$$

This energy is better than that obtained with a single determinant wave function like Ψ_{HF} , *i.e.*, -1.1167143 a.u., but still lies far from the best energy[6] of the ground state of the hydrogen molecule $E_{H_2} = -1.1744757$ a.u. One obvious reason for this discrepancy is the poor representation of the atomic orbitals used in our calculation. Nevertheless, recall that

Heinemann, Kolb and Fricke[7] have estimated the best Hartree-Fock(HF) energy of H_2 in -1.1336296 a.u., at $R = 1.4$ a.u. Inspection of these numbers suggests that there remain problems in the HF representation of interacting electrons that stretch beyond the limits of the method itself.

Electron correlation is *vaguely* defined as the difference between the one determinant HF representation of the interacting system and its exact representation.

From the previous discussion it is now made clear that there are more than one source of electron correlation. Thus, for the stretched H_2 the effect of electron correlation is to eliminate the ionic configurations from the HF wave function. When the hydrogen atoms approach at shorter distances electron correlation has more subtle effects and are more difficult to account for.

These two type of effects illustrate the two types of electron correlation that we shall deal with. The former, called *non-dynamical* correlation relates to the degeneracy of bonding and antibonding configurations. Therefore, they will interact strongly and hence cannot be treated in isolation from each other. Observe that for $R \rightarrow \infty$, the two determinants of Eq. (5) have the same energy, E_H . The non-dynamical electron correlation is consequently system-specific.

The latter, due to short range interactions between the electrons, stems from the failure of the HF representation to describe the detailed correlated motion of the electrons as induced by their instantaneous mutual repulsion. This type of electron correlation is customarily referred to as *dynamical* correlation and, since it is non-specific is, in a sense, universal.

Unfortunately the field is plagued with a number of terms to denote the same concept. This can be best illustrated by referring to the energies and occupation numbers of the orbitals of H_2 for three internuclear distances. As shown in Table 1, at the equilibrium distance, the $1\sigma_g$ orbital with an occupation of 1.9643 should provide a reasonable representation of the exact wave function. Nevertheless, the $1\sigma_u$ orbital with an occupation of 0.0199 is the second largest populated orbital. This orbital has a nodal plane which bisect the molecular axis. Its occupation, therefore, increases the probability of finding the two electrons on one nucleus each. This, which is non-dynamical correlation, is often referred to as *left-right correlation*[8]. The $1\pi_u$ orbital, which has an occupation of 0.0043 at the equilibrium distance, possesses a nodal plane which contains the molecular axis. Then its occupation increases the probability of finding the electrons on opposite sides of the molecular axis. This is normally referred to as *angular correlation*[9]. Notice finally that the $2\sigma_g$ orbital belongs to the same irreducible representation as the most populated orbital $1\sigma_g$, but it has a radial node. Occupation of this orbital introduces *radial correlation*,

TABLE 1. Energies, a.u., and occupations of a number of selected natural orbitals of H_2

	$R=1.4$ a.u.	$R=4.0$ a.u.	$R=15.0$ a.u.
E_{H_2}	-1.173796	-1.015724	-0.999891
$n(1\sigma_g)$	1.9643	1.5162	1.0000
$n(2\sigma_g)$	0.0061	0.0015	0.0000
$n(1\sigma_u)$	0.0199	0.4804	1.0000
$n(2\sigma_u)$	0.0002	0.0000	0.0000
$n(1\pi_u)$	0.0043	0.0000	0.0000

increasing the probability of locating electrons at different distances along the molecular axis.

The discussion of preceding paragraph points to an alternative viewpoint to look at the electron correlation problem. Indeed, electron correlation, as shown above, has to do with probabilities and densities of the electron pairs. Thus, in addition to the energy based studies, electron-pair distributions yield insight to afford quantitative assessment of the short- and long-range effects of electron-electron interaction in a given system. In particular, the electron intracule $I(\mathbf{u})$ and extracule $E(\mathbf{R})$ densities, as well as their corresponding spherical averages, $h(u)$ and $d(R)$, are genuine electron-pair densities useful to characterize the motion of a pair of electrons in atoms and molecules[10]. For a system of N electrons, the intracule density and its spherical averaged density are defined by

$$\begin{aligned} I(\mathbf{u}) &= \sum_{i<j} \langle \Psi | \delta(\mathbf{u} - \mathbf{r}_i + \mathbf{r}_j) | \Psi \rangle \\ &= \int \Gamma_2(\mathbf{r}_1, \mathbf{r}_2) \delta(\mathbf{u} - \mathbf{r}_1 + \mathbf{r}_2) d\mathbf{r}_1 d\mathbf{r}_2 \end{aligned} \quad (8)$$

and

$$h(u) = \frac{1}{4\pi} \int d\Omega_u I(\mathbf{u}) \quad (9)$$

whereas the extracule densities are:

$$E(\mathbf{R}) = \int \Gamma_2(\mathbf{r}_1, \mathbf{r}_2) \delta\left(\mathbf{R} - \frac{\mathbf{r}_1 + \mathbf{r}_2}{2}\right) d\mathbf{r}_1 d\mathbf{r}_2 \quad (10)$$

and

$$d(R) = \frac{1}{4\pi} \int d\Omega_R E(\mathbf{R}) \quad (11)$$

where $\Gamma_2(\mathbf{r}_1, \mathbf{r}_2) = (N(N-1)/2) \int |\Psi(\mathbf{r}_1, \mathbf{r}_2, \dots, \mathbf{r}_N)|^2 d\mathbf{r}_3 \dots d\mathbf{r}_N$ is the spin-less electron pair density and δ denotes the Dirac's delta function. They represent the probability density functions for the relative electron-pair vector $(\mathbf{r}_i - \mathbf{r}_j)$ and the center of mass electron-pair vector $(\mathbf{r}_i + \mathbf{r}_j)/2$ to be at \mathbf{u} and \mathbf{R} , respectively. Their genuine two-electron character combined with the low dimensionality make these functions ideally suited to unveil the nature of electron-electron interaction in an elegant and intelligible manner.

The connection between the two viewpoints alluded to above can be established as follows. The time independent Schrödinger equation for our N electron system

$$\hat{H}\Psi(\mathbf{r}_1, \mathbf{r}_2, \dots, \mathbf{r}_N) = E\Psi(\mathbf{r}_1, \mathbf{r}_2, \dots, \mathbf{r}_N) \quad (12)$$

can also be expressed in terms of the one- and two-electron density functions as

$$\begin{aligned} E &= T + E_{eN} + E_{ee} \\ &= \int d\mathbf{r} \frac{-\nabla_{\mathbf{r}}^2}{2} \gamma(\mathbf{r}, \mathbf{r}') \Big|_{\mathbf{r}'=\mathbf{r}} + \int d\mathbf{r} \rho(\mathbf{r}) V_{eN}(\mathbf{r}) \\ &+ \int d\mathbf{r} \int d\mathbf{r}' \frac{\Gamma_2(\mathbf{r}, \mathbf{r}')}{|\mathbf{r} - \mathbf{r}'|} \end{aligned} \quad (13)$$

The one particle density matrix is given by

$$\gamma(\mathbf{r}, \mathbf{r}') = N \int \Psi(\mathbf{r}, \mathbf{r}_2, \dots, \mathbf{r}_N) \Psi(\mathbf{r}', \mathbf{r}_2, \dots, \mathbf{r}_N) d\mathbf{r}_2 \dots d\mathbf{r}_N \quad (14)$$

and the electron density function is

$$\rho(\mathbf{r}) = \gamma(\mathbf{r}, \mathbf{r}) = \sum_{i=1}^N \langle \Psi | \delta(\mathbf{r} - \mathbf{r}_i) | \Psi \rangle \quad (15)$$

The electron pair density accounts for the probability $\Gamma_2(\mathbf{r}_1, \mathbf{r}_2) d\mathbf{r}_1 d\mathbf{r}_2$ of one electron being in the volume $d\mathbf{r}_1$ around \mathbf{r}_1 when other electron is known to be in the volume $d\mathbf{r}_2$ around \mathbf{r}_2 . If the electrons were independent[11], clearly: $\Gamma_2(\mathbf{r}_1, \mathbf{r}_2) = \rho(\mathbf{r}_1)\rho(\mathbf{r}_2)$. Therefore, it is then intuitive that for correlated electrons, an *exchange-correlation* contribution which takes into account all kinds of correlations between the electrons must be added to the uncorrelated case. Thus,

$$\Gamma_2(\mathbf{r}_1, \mathbf{r}_2) = \frac{1}{2} \rho(\mathbf{r}_1) [\rho(\mathbf{r}_2) + \rho_{xc}(\mathbf{r}_1, \mathbf{r}_2)] \quad (16)$$

Substituting Eq. (16) into the last term of the right hand side of Eq. (13) we obtain that the electron–electron repulsion energy can be expressed as

$$E_{ee} = J[\rho] + E_{xc}[\rho] = \frac{1}{2} \int d\mathbf{r}d\mathbf{r}' \frac{\rho(\mathbf{r})\rho(\mathbf{r}')}{|\mathbf{r} - \mathbf{r}'|} + \frac{1}{2} \int d\mathbf{r}d\mathbf{r}' \frac{\rho(\mathbf{r})\rho_{xc}(\mathbf{r}, \mathbf{r}')}{|\mathbf{r} - \mathbf{r}'|} \quad (17)$$

And finally, also substituting Eq. (16) now into Eq. (8) we obtain that

$$I(\mathbf{u}) = \frac{1}{2} \int d\mathbf{r} \rho(\mathbf{r})\rho(\mathbf{r} + \mathbf{u}) + \frac{1}{2} \int d\mathbf{r} \rho(\mathbf{r})\rho_{xc}(\mathbf{r}, \mathbf{r} + \mathbf{u}) \quad (18)$$

Recall at this point that Hohenberg and Kohn demonstrated in their *Density Theory Functional* (DFT) foundational paper[12], that all properties of interacting electron systems are completely determined by its ground state electron density, $\rho(\mathbf{r})$. This includes, the energy of the ground state, the energies of the excited states, response properties, etc. Therefore, ρ_{xc} itself must also be a functional of the ground state electron density in accordance with Eq. (13), although its exact form has been proved difficult to find out, as it will be illustrated in Section 2.

2. The exchange-correlation hole density for stretched H_2

We will demonstrate one practical realization of Eq. (16) to estimate the exchange-correlation hole density for the dissociated H_2 . The exact wave function, Eq. (1), allows the calculation of the necessary ingredients of Eq. (16) to obtain ρ_{xc} directly. Thus, clearly, the diagonal of the second-order density matrix is simply the square of the wave function itself,

$$\begin{aligned} \Gamma_2(\mathbf{r}, \mathbf{r}') &= \frac{2(2-1)}{2} |\Psi_{HL}(\mathbf{r}, \mathbf{r}')|^2 \\ &= \frac{1}{2} [\psi_A(\mathbf{r})\psi_B(\mathbf{r}') + \psi_A(\mathbf{r}')\psi_B(\mathbf{r})]^2 \end{aligned} \quad (19)$$

and the electron density is also simple:

$$\begin{aligned} \rho(\mathbf{r}) &= 2 \int |\Psi_{HL}(\mathbf{r}, \mathbf{r}_2)|^2 d\mathbf{r}_2 \\ &= \psi_A^2(\mathbf{r}) + \psi_B^2(\mathbf{r}) \end{aligned} \quad (20)$$

Hence substituting Eq.'s (19) and (20) into Eq. (16) we obtain that

$$\rho_{xc}(\mathbf{r}, \mathbf{r}') = - \frac{\psi_A^2(\mathbf{r})\psi_A^2(\mathbf{r}') + \psi_B^2(\mathbf{r})\psi_B^2(\mathbf{r}')}{\rho(\mathbf{r})} \quad (21)$$

which gives the spherically averaged exchange-correlation hole density as,

$$\begin{aligned}\tilde{\rho}_{xc}(\mathbf{r}, u) &= \frac{1}{4\pi} \int d\Omega_{\mathbf{u}} \rho_{xc}(\mathbf{r}, \mathbf{r} + \mathbf{u}) \\ &= -\frac{\psi_A^2(\mathbf{r}) \int d\Omega_{\mathbf{u}} \psi_A^2(\mathbf{r} + \mathbf{u}) + \psi_B^2(\mathbf{r}) \int d\Omega_{\mathbf{u}} \psi_B^2(\mathbf{r} + \mathbf{u})}{4\pi \rho(\mathbf{r})}\end{aligned}\quad (22)$$

The solution of Eq. (22) requires the evaluation of the following integral

$$\begin{aligned}\int d\Omega_{\mathbf{u}} \psi_{A,B}^2(\mathbf{r} + \mathbf{u}) &= 2\pi \int_{-1}^1 d\mu \frac{1}{\pi} e^{2|\mathbf{r} + \mathbf{u} \pm \mathbf{R}/2|} \\ &= \frac{e^{-2|\mathbf{r} \pm \mathbf{R}/2| - u} (1 + 2|\mathbf{r} \pm \mathbf{R}/2| - u)}{2|\mathbf{r} \pm \mathbf{R}/2| u} \\ &\quad - \frac{e^{-2|\mathbf{r} \pm \mathbf{R}/2| + u} (1 + 2|\mathbf{r} \pm \mathbf{R}/2| + u)}{2|\mathbf{r} \pm \mathbf{R}/2| u}\end{aligned}\quad (23)$$

which arises from the orbitals, $\psi_{A,B}(\mathbf{r}) = \exp(-|\mathbf{r} \pm \mathbf{R}/2|)/\sqrt{\pi}$. Hence, the plus sign in the right hand side of Eq. (23) corresponds to orbital ψ_A and the minus sign to orbital ψ_B . Finally using Eq. (23) in Eq. (22), the exchange-correlation hole density can be cast as,

$$\begin{aligned}\tilde{\rho}_{xc}(\mathbf{r}, u) &= -\frac{e^{-2u_{>}^+}}{\pi 2u_{>}^+} \left[(1 + 2u_{>}^+) \frac{\sinh(2u_{<}^+)}{2u_{<}^+} - 2 \cosh(2u_{<}^+) \right] \\ &\quad - \frac{e^{-2u_{>}^-}}{\pi 2u_{>}^-} \left[(1 + 2u_{>}^-) \frac{\sinh(2u_{<}^-)}{2u_{<}^-} - 2 \cosh(2u_{<}^-) \right]\end{aligned}\quad (24)$$

where $u_{>}^{\pm} = \max\{u, |\mathbf{r} \pm \mathbf{R}/2|\}$ and $u_{<}^{\pm} = \min\{u, |\mathbf{r} \pm \mathbf{R}/2|\}$. One important property of the exchange-correlation hole density is its sum rule, namely,

$$\int d\mathbf{r} \rho_{xc}(\mathbf{r}, \mathbf{r}') = -1, \quad \forall \mathbf{r} \quad (25)$$

so that the spherically averaged exchange-correlation hole density, must satisfy the following integral equation:

$$4\pi \int_0^{\infty} du u^2 \tilde{\rho}_{xc}(\mathbf{r}, u) = -1, \quad \forall \mathbf{r} \quad (26)$$

Integration of Eq. (24) confirms that our exchange-correlation hole density meets the requirement imposed in Eq. (26).

The system averaged exchange-correlation hole density is

$$4\pi \int d\mathbf{r} \rho(\mathbf{r}) \tilde{\rho}_{xc}(\mathbf{r}, u) = -\frac{e^{-2u}}{12\pi} (4u^2 + 6u + 3) \quad (27)$$

and consequently, the exchange correlation energy, recall Eq. (17), turns out to be

$$E_{xc} = 2\pi \int d\mathbf{r} \rho(\mathbf{r}) \int_0^\infty du u \tilde{\rho}_{xc}(\mathbf{r}, u) = -\frac{5}{8} \quad (28)$$

In order to calculate the total energy of our stretched H_2 molecule we still need values for $J[\rho]$, and T and E_{eN} , see Eq.'s (13) and (17). The calculation of $J[\rho]$ is a textbook exercise which is easily achieved by using the Fourier transform of $|\mathbf{r} - \mathbf{r}'|^{-1}$, *i.e.*:

$$\frac{1}{|\mathbf{r} - \mathbf{r}'|} = \frac{1}{2\pi^2} \int d\mathbf{k} \frac{e^{-i\mathbf{k}\cdot(\mathbf{r}-\mathbf{r}')}}{k^2} \quad (29)$$

The final result is

$$\begin{aligned} J[\rho] &= \frac{1}{2\pi^4} \int d\mathbf{r} d\mathbf{r}' d\mathbf{k} \frac{1}{k^2} e^{-2(r+r')-i\mathbf{k}\cdot(\mathbf{r}-\mathbf{r}')} \\ &= \frac{1}{2\pi^4} \int d\mathbf{k} \frac{1}{k^2} \frac{2^8 \pi^2}{(4+k^2)^4} = \frac{5}{8} \end{aligned} \quad (30)$$

Consequently, in accordance with Eq. (13), the total energy is

$$\begin{aligned} E &= \int d\mathbf{r} \frac{-\nabla_{\mathbf{r}}^2}{2} \psi_A(\mathbf{r}) \psi_A(\mathbf{r}')|_{\mathbf{r}=\mathbf{r}'} + \int d\mathbf{r} \frac{-\nabla_{\mathbf{r}}^2}{2} \psi_B(\mathbf{r}) \psi_B(\mathbf{r}')|_{\mathbf{r}=\mathbf{r}'} \\ &+ \int d\mathbf{r} [\psi_A^2(\mathbf{r}) + \psi_B^2(\mathbf{r})] \left(\frac{-1}{|\mathbf{r} + \mathbf{R}/2|} + \frac{-1}{|\mathbf{r} - \mathbf{R}/2|} \right) \\ &= 2T_{\text{H}} + 2E_{eN,\text{H}} = 2E_{\text{H}} \end{aligned} \quad (31)$$

where E_{H} stands for the energy of a hydrogen atom. Eq. (31), therefore, renders the correct dissociation limit of H_2 .

The spherically averaged exchange-correlation hole density of Eq. (24), is plotted in Figure 1 as a function of the distance of the reference electron to one of the two nuclei, $|\mathbf{r} \pm \mathbf{R}/2|$ and the interelectronic distance u .

Observe that any of the forms of the exchange-correlation hole density written up to now, see Eq.'s (21)-(27), are difficult to cast into a form involving only the electron density $\rho(\mathbf{r})$, as we announced at the bottom of Section 1.

Nevertheless, the close relation existing between the exchange-correlation density and the electron pair density as suggested by Eq. (16), puts forward the very important hidden supporting role played by electron pair densities in DFT, toward a rational and physically sound designing of approximate exchange-correlation densities. This point has been recently illustrated very elegantly by Maitra and Burke[13] by showing how the elementary properties of the electron pair density suffice to determine approximate but

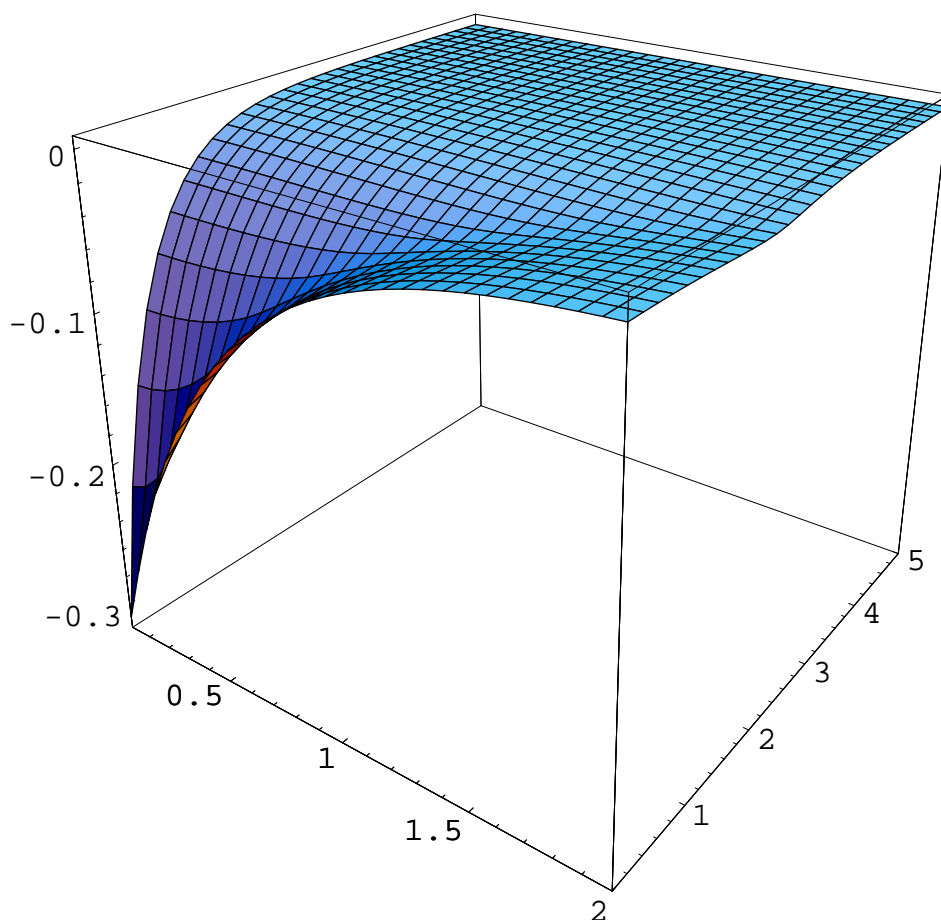


Figure 1. Spherically averaged exchange hole for the hydrogen molecule H_2 , as a function of the distance of the reference electron with respect to the nucleus, $|\mathbf{r} \pm \frac{\mathbf{R}}{2}| = 0 - 2$ a.u. and the interelectronic distance, $u = 0 - 5$ a.u.

accurate exchange and correlation functionals. Hence, in the following sections we will discuss some of the important properties of the two electron pair functions defined earlier, *i.e.*: the intracule density and the extracule density.

3. Properties of the Intracule Density

The electron density, $\rho(\mathbf{r})$ has been widely more studied than the electron pair densities, not only because $\rho(\mathbf{r})$ is the key quantity of DFT, but also because, the reduction of the total N -electron wave function to $\rho(\mathbf{r})$ is easier

than the reduction to either $I(\mathbf{u})$ or $E(\mathbf{R})$.

However, in the last decade, a new set of algorithms and computational procedures for evaluating the molecular integrals associated to the pair densities have become available, and some of them have been reviewed recently[10].

In particular, progress in the field has been led by Gill *et al.*[14], who have extended the PRISM algorithm using tensor multiplication rules and its associativity to evaluate efficiently the matrix elements for both the intracule and extracule densities. Additionally, one more landmark development for the accurate and efficient calculation of the pair densities was carried out by Cioslowski *et al.*[15]. His procedure is based on the fact that both $I(\mathbf{u})$ and $E(\mathbf{R})$ can be expressed as expectation values of two-electron operators, thus both being first-order, two-electron response properties amenable to the energy-derivative formalism that has been utilized with great success in calculations of energy gradients in electron correlation methods[16]. The versatility of these approaches make routine calculations on intracule and extracule densities feasible at any level of theory.

3.1. THE INTRACULE DENSITY OF THE HYDROGEN MOLECULE

For the Hartree-Fock wave function of H_2 of Eq. (3), the Slater-Condon rules for matrix elements of two-electron operators between one-determinant wave functions can be used to write Eq. (8) as follows:

$$\begin{aligned} I_{HF}(\mathbf{u}) &= \frac{1}{2} \sum_{m,n}^N ([mm | \delta(\mathbf{u} - \mathbf{r}_1 + \mathbf{r}_2) | nn] \\ &\quad - [mn | \delta(\mathbf{u} - \mathbf{r}_1 + \mathbf{r}_2) | nm]) \end{aligned} \quad (32)$$

In this equation we have used the notation of Szabo and Ostlund[17]. By introducing the usual definition of the elements of the density matrix in the Roothaan-Hall self-consistent field method for a closed shell,

$$P_{\nu\mu} = 2 \sum_i^{N/2} C_{\nu i} C_{\mu i}^* \quad (33)$$

the intracule density can be written as follows:

$$I_{HF}(\mathbf{u}) = \sum_{\nu\mu\lambda\sigma} \left(\frac{1}{2} P_{\nu\mu} P_{\lambda\sigma} - \frac{1}{4} P_{\lambda\mu} P_{\nu\sigma} \right) J_{\nu\mu\lambda\sigma}(\mathbf{u}) \quad (34)$$

in terms of the basic intracule two-electron integrals

$$J_{\nu\mu\lambda\sigma}(\mathbf{u}) = (\nu\mu | \delta(\mathbf{u} - \mathbf{r}_1 + \mathbf{r}_2) | \lambda\sigma) \quad (35)$$

Similarly for the Heitler-London ansatz of wave function, Eq. (5), which will be referred to as *Configuration Interaction* (CI) hereafter, the Slater-Condon rules yield

$$I_{CI}(\mathbf{u}) = \sum_{\nu\mu\lambda\sigma} \left(\frac{1}{2} P_{\nu\mu} P_{\lambda\sigma} - \frac{1}{4} P_{\lambda\mu} P_{\nu\sigma} \right. \\ \left. + c P_{\sigma\mu} C_{\nu 2}^* C_{\lambda 2} + c^2 C_{\mu 2}^* C_{\nu 2} C_{\sigma 2}^* C_{\lambda 2} \right) J_{\nu\mu\lambda\sigma}(\mathbf{u}) \quad (36)$$

For *s*-type Gaussian basis function the evaluation of Eq. (35) is straightforward. Namely, its can be cast as,

$$J_{\nu\mu\lambda\sigma}(\mathbf{u}) = \frac{K \mathcal{J}}{(2\pi)^3} \quad (37)$$

with

$$K = \exp \left(-\frac{\nu\mu}{\nu+\mu} |\mathbf{R}_A - \mathbf{R}_B|^2 - \frac{\lambda\sigma}{\lambda+\sigma} |\mathbf{R}_C - \mathbf{R}_D|^2 \right) \quad (38)$$

arising from the contraction of the ν and μ gaussians centered respectively on \mathbf{R}_A and \mathbf{R}_B , to the center \mathbf{R}_P and likewise for λ and σ to \mathbf{R}_Q . The integral \mathcal{J} is:

$$\mathcal{J} = \int d\mathbf{r}_1 d\mathbf{r}_2 d\mathbf{k} e^{-i\mathbf{k}\cdot(\mathbf{u}-\mathbf{R}_P+\mathbf{R}_Q)} e^{-i\mathbf{k}\cdot(\mathbf{r}_1-\mathbf{R}_P)-\gamma_1|\mathbf{r}_1-\mathbf{R}_P|^2} \\ e^{-i\mathbf{k}\cdot(\mathbf{r}_2-\mathbf{R}_Q)-\gamma_2|\mathbf{r}_2-\mathbf{R}_Q|^2} \quad (39)$$

with $\gamma_1 = \nu + \mu$ and $\gamma_2 = \lambda + \sigma$ and where we have used the Fourier transform representation for the Dirac's delta function,

$$\delta(\mathbf{u} - \mathbf{r}_1 + \mathbf{r}_2) = \left(\frac{1}{2\pi} \right)^3 \int d\mathbf{k} e^{-i\mathbf{k}\cdot(\mathbf{u}-\mathbf{r}_1+\mathbf{r}_2)} \quad (40)$$

The integrals over \mathbf{r}_1 and \mathbf{r}_2 in Eq. (39) are easy and yield

$$\int d\mathbf{r}_1 e^{-i\mathbf{k}\cdot(\mathbf{r}_1-\mathbf{R}_P)-\gamma_1|\mathbf{r}_1-\mathbf{R}_P|^2} = 2\pi \int_0^\infty dr_1 r_1^2 e^{-\gamma_1 r_1^2} \int_{-1}^1 d\theta e^{-ikr_1\theta} \\ = \frac{4\pi}{k} \int_0^\infty dr_1 \sin(kr_1) r_1 e^{-\gamma_1 r_1^2} \\ = \left(\frac{\pi}{\gamma_1} \right)^{3/2} e^{-\frac{k^2}{4\gamma_1}} \quad (41)$$

and likewise for \mathbf{r}_2 . Therefore,

$$\mathcal{J} = \left(\frac{\pi^2}{\gamma_1 \gamma_2} \right)^{3/2} \int d\mathbf{k} e^{-i\mathbf{k}\cdot(\mathbf{u}-\mathbf{R}_P+\mathbf{R}_Q)} e^{-4k^2/\Delta} \quad (42)$$

with $\Delta = \gamma_1\gamma_2/(\gamma_1 + \gamma_2)$. The integral of Eq. (42) has the same functional form as that of Eq. (41), hence, it can be solved likewise. The final result is:

$$J_{\nu\mu\lambda\sigma}(\mathbf{u}) = K \left(\frac{\pi}{\gamma_1 + \gamma_2} \right)^{3/2} e^{-\Delta|\mathbf{u}-\mathbf{R}_P+\mathbf{R}_Q|^2} \quad (43)$$

and the spherically averaged basic intracule integral

$$J_{\nu\mu\lambda\sigma}(u) = \frac{1}{4\pi} \int d\Omega_{\mathbf{u}} J_{\nu\mu\lambda\sigma}(\mathbf{u}) \quad (44)$$

is

$$J_{\nu\mu\lambda\sigma}(u) = K \left(\frac{\pi}{\gamma_1 + \gamma_2} \right)^{3/2} e^{-\Delta(u^2+R_{PQ}^2)} \frac{\sinh(2R_{PQ}\Delta u)}{2R_{PQ}\Delta u} \quad (45)$$

where $R_{PQ}=|\mathbf{R}_P - \mathbf{R}_Q|$.

Combining Eq.'s (32), (34) and (36) with Eq. (45) we can readily calculate the intracule probability distributions $4\pi u^2 h(u)$, of H_2 as a function of both the interelectronic distance u and the internuclei separation R . Figure (2) illustrates these probability distributions for both the HF (restricted and unrestricted) and CI representations of the electronic wave function as the internuclear distance stretches as calculated by Boyd *et al.*[18]. Observe the different dissociation depicted by each of the wave functions.

Thus, for the CI representation of the wave function the probability of the interelectronic distance follows closely to the internuclear distance. This is very supportive of the homolitic dissociation of the bond, where each nucleus gets one electron.

For the RHF representation, however, at large internuclear distances, *i.e.*: $R=15$ a.u., the probability of finding the electron pair both, with the electrons close to each other and at interelectronic distances similar to the internuclear separation is large. This odd behavior of the restricted HF wave function is *corrected* by lifting the constraint relative to the equal spatial distribution of the orbitals imposed by the RHF determinant. Removal of such a constrain leads to the unrestricted solution, which for $R \geq 2.3$ a.u. has lower energy than the RHF solution of the HF equations. Recall that at internuclear distances $R \geq 2.3$ a.u the RHF becomes unstable[5]

We already knew that. However, notice that it is only at this point that we have been able to follow, for the first time, the dissociation process of the electron pair in full detail, just looking at the intracule density.

Inspection of the intracule density might also serve to unveil some *counterintuitive* electron correlation effects like the unusual behavior of the interelectronic repulsion in the $^3\Pi_u$ excited state of H_2 reported by Tal and Katriel[19]. For a diatomic molecule as the nuclei pull apart electrons are expected to increase their mean interelectronic separation. This is the usual

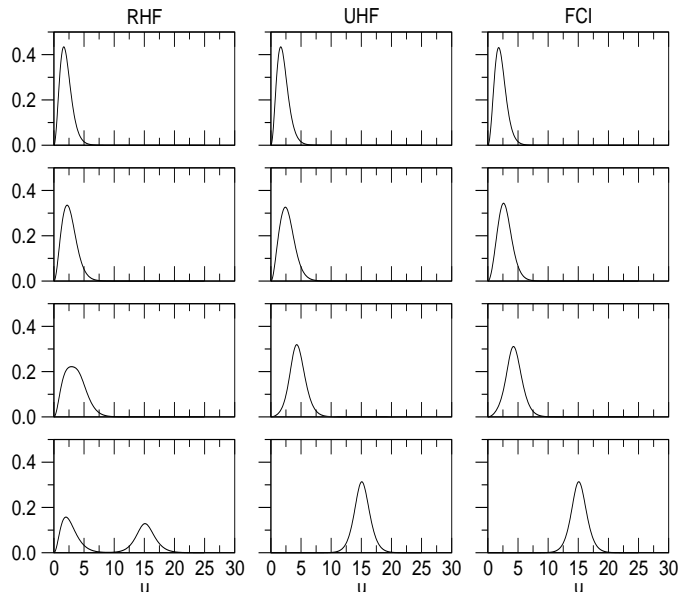


Figure 2. The electron pair probability distribution, $4\pi u^2 h(u)$, in the $^1\Sigma_g^+$ ground state of H_2 for four internuclear separations, from top to bottom $R=1.4$ a.u., $R=2.4$ a.u., $R=4.0$ a.u. and $R=15.0$ a.u. The graph on the left hand side corresponds to the RHF wave function, the one on the right hand side to the FCI wave function and the one in the middle to the UHF wave function.

behavior of most investigated states of H_2 , except for the first $^3\Pi_u$ excited state. For this state an initial decrease of the mean interelectronic separation is observed as nuclei stretch. The calculated mean interelectronic separations of Tal and Katriel were based on a rather crude HF wave function with a small basis set consisting of four uncontracted sp primitives. One, therefore, is tempted to ascribe this *odd* behavior of the mean interelectronic distance to the crudeness of the calculation, although in their paper Tal and Katriel argue that "...the non-monotonic trend is real rather than a Hartree-Fock artifact."

We have calculated the spherically averaged intracuclear density for both the $^3\Pi_u$ and the $^1\Pi_u$ states of H_2 from an accurate *Full Configuration Interaction* (FCI) wave function constructed from a large Gaussian basis set. The energies of the states studied are shown in Table 2 and compared with the benchmark results of Rothenberg and Davidson[20]. Data shown Table 2 is very supportive of the accuracy of our wave functions. The calculated mean

TABLE 2. Energies, a.u., mean internuclear repulsion energy, in a.u., mean interelectronic separation, in a.u. and electron-electron coalescence for two excited states of H_2 , at two selected internuclear separations, R in a.u. In *italics* the energies of Rothenberg and Davidson are shown

R	$-E$	$\langle u^{-1} \rangle$	$\langle u \rangle$	$I(0)$
$^1\Pi$				
1.95	0.717946 <i>0.717965</i>	0.217651	5.67413	0.008052
2.05	0.717458 <i>0.717439</i>	0.215855	5.711587	0.007728
$^3\Pi$				
1.95	0.737260 <i>0.736977</i>	0.241831	4.971931	0.00
2.05	0.736854 <i>0.736455</i>	0.239319	5.013047	0.00

values of the intracuclear coordinate u are shown in Figure 3 as a function of the internuclear separation. The non-monotonic behavior of both the mean interelectronic repulsion energy and the mean interelectronic separation as a function of R of the $^3\Pi_u$ state, in sharp contrast with the monotonic behavior observed in the $^1\Pi_u$ state, is clearly seen from the inspection of the graphs. This confirms that the unusual behavior of the electron pair in the $^3\Pi_u$ state of H_2 is not due the inaccuracy of the HF wave function. Inspection of the difference between the intracuclear probability distribution functions for calculated at two internuclear distances provides an alternative view of these unusual correlation effects. Indeed, as seen in Figure 4, we observed that for the $^1\Pi_u$ state, increasing the internuclear distance from $R = 0.5$ a.u. to $R = 0.75$ a.u. and from $R = 1.5$ a.u to $R = 1.95$ a.u. results in an increased probability of finding the electron pair at larger distances. Notice that the two curves of the upper graph of Figure 4 are positive for small interelectronic distances, hence the probability of finding an electron pair with this sort interelectronic distance is larger in this region, and vice-versa for large interelectronic distances.

However, for the $^3\Pi_u$ state, the probability of finding the electron close together is larger for $R = 0.75$ a.u. than for $R = 0.5$ a.u. Namely, increasing the internuclear distance from $R = 0.5$ a.u. to $R = 0.75$ a.u. increases the probability of finding the electrons at smaller interelectronic distances. This behavior is *counterintuitive*. The main difference between the $^1,^3\Pi_u$ states arises from the symmetry of the spatial part of the wave function. Since,

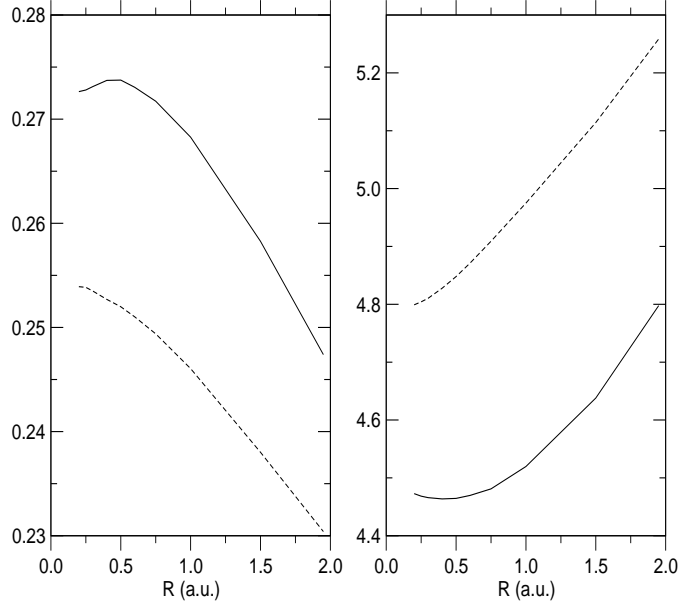


Figure 3. Dependence of the mean interelectronic repulsion energy (left hand side graph) and the mean interelectronic separation (right hand side graph) in the $^3\Pi_u$ state (solid curve) and in the $^1\Pi_u$ state (dashed curve).

the triplet spin wave function is symmetric, its associated spatial part must be antisymmetric under exchange of electrons, whereas for the singlet the antisymmetry of the spin wave function dictates that the spatial part must be symmetric under exchange of electrons. One immediate consequence of this is that the intracuclear density must be zero at $\mathbf{u}=0$ for the triplet state. Recall that the for an antisymmetric function, like the spatial part of the triplet state,

$$\Psi(\mathbf{r}_1, \mathbf{r}_2) = -\Psi(\mathbf{r}_2, \mathbf{r}_1) \quad (46)$$

Hence, for $\mathbf{r}_1 = \mathbf{r}_2$, we obtain that

$$\Psi(\mathbf{r}_1, \mathbf{r}_1) = 0, \quad \forall \mathbf{r}_1 \quad (47)$$

Therefore,

$$I(0) = \langle \Psi | \delta(\mathbf{r}_1 - \mathbf{r}_2) | \Psi \rangle$$

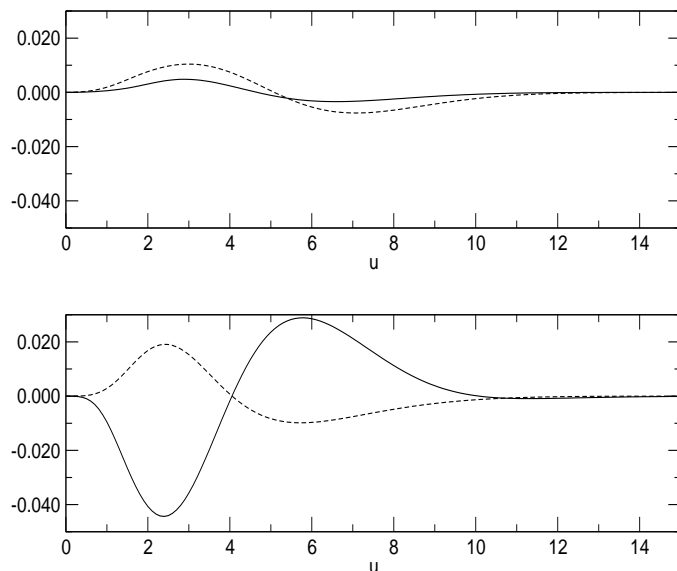


Figure 4. Difference of the intracule probability function for the ${}^1\Pi_u$ state (upper graph) and for the ${}^3\Pi_u$ state (bottom graph). Solid curve: $I(u; R = 0.5) - I(u; R = 0.75)$ and dashed curve: $I(u; R = 1.5) - I(u; R = 1.95)$

$$\begin{aligned}
 &= \int d\mathbf{r}_1 d\mathbf{r}_2 \Psi^*(\mathbf{r}_1, \mathbf{r}_2) \Psi(\mathbf{r}_1, \mathbf{r}_2) \delta(\mathbf{r}_1 - \mathbf{r}_2) \\
 &= \int d\mathbf{r}_1 \Psi^*(\mathbf{r}_1, \mathbf{r}_1) \Psi(\mathbf{r}_1, \mathbf{r}_1) = 0
 \end{aligned} \tag{48}$$

Our explicitly calculated values of $I(0)$ for the ${}^3\Pi_u$ state, shown in Table 2 agree with this prediction.

However, due to the continuity of the intracule density function, it is expected that the spherically averaged intracule probability function, namely

$$4\pi u^2 h(u) = u^2 \int d\Omega_u I(\mathbf{u}) \tag{49}$$

will start building up slower in the triplet state than in the singlet, because in the singlet state $I(0) \neq 0$. Consequently one expects that the probability of finding an electron pair at short interelectronic distances will be larger for the singlet than for the triplet. The intracule probability function differences plotted in Figure 5 confirm this assumption. $4\pi u^2 h(u)$ for the triplet

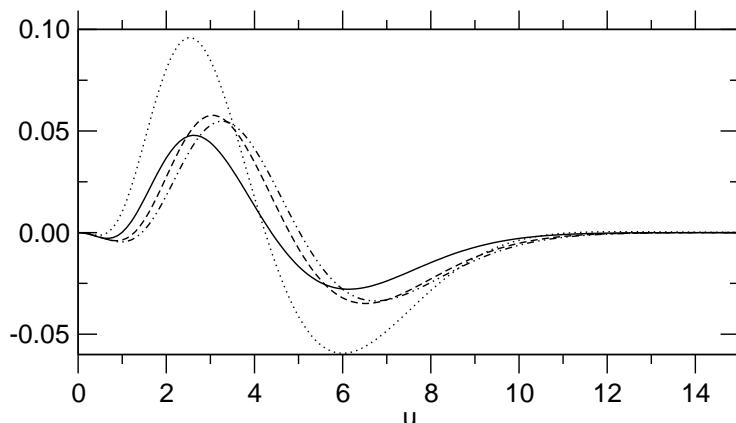


Figure 5. Difference between the intracuclear probability functions of the $^3\Pi_u$ state and the $^1\Pi_u$ state. Solid curve: $R = 0.5$ a.u. Dotted curve $R = 0.75$ a.u. Dashed curve: $R = 1.5$ a.u. Dotted and dashed curve: $R = 1.95$ a.u.

is smaller than for the singlet, hence the negative values shown in Figure 5 at short interelectronic distances u for all the internuclear distances investigated. This has been argued to be the physical basis of the well-known Hund's rule. Namely, the lower probability of finding electron pairs close together in the triplet with respect to the singlet results in a greater electron repulsion in the low spin state as compared to the high spin state and, consequently, the high spin state should be more stable. Numerous calculations on a variety of systems (see page 234 of Ref.[10] for a full list of references) and our own ones reported in Table 2 showed, however, that this textbook explanation is invalid. The electron repulsion energy is larger for the $^3\Pi_u$ state than for the $^1\Pi_u$ state. The physical basis for the larger stability of the triplet with respect to the singlet is, nevertheless, insinuated in Figure 5. Notice that although the probability of finding an electron pair close together is smaller in the triplet than in the singlet, the triplet favors clearly intermediate interelectronic distances as compared to the singlet state, for the probability of finding an electron pair with large interelectronic distance is larger in the singlet than in the triplet. This can only be if the electron cloud is more compact in the triplet than in the singlet and, consequently, the electron-nucleus attraction energy is larger in the triplet than in the singlet so that it overweighs the larger electron repulsion of the latter[21, 22, 23, 24].

In other words, since the electrons of the triplet avoid each other in

the vicinity of the nuclei they screen less the nuclear charge and, consequently the electron cloud gets more compact than in the singlet for which the nuclear charge is screened more efficiently. This leads ultimately to an increased electron nucleus attraction for the triplet, which overweighs the larger electron repulsion of the triplet yielding, therefore, a more stable triplet state.

For other systems, although the topology of both $I(\mathbf{u})$ and $E(\mathbf{R})$ is considerably more complex than that of the more familiar electron density $\rho(\mathbf{r})$, considerable progress has been achieved over the last two decades. Thus, it has become possible to identify different *classes* of electron–electron interactions and find the regions of the intracule or extracule space to which they contribute[25, 26, 27, 28, 29]. It also allows the introduction of the concept of the *correlation cage*[30], as the domain in the space of inter-electronic distance vectors contained within the sphere on whose surface the intracule density is locally a maximum and encapsulates the electron–electron coalescence point. The shape and size of the correlation cage has been found to be entirely determined by the topological properties of the intracule density[30, 31], thus avoiding any references to ill-defined *uncorrelated* quantities.

A further step towards the simplified description of electron pair properties is the use of the electron–electron coalescence and counterbalance densities. Indeed, these two functions inherit the electron pair character and are conveniently defined in the usual real \mathbf{r} -space. The electron–electron coalescence[32, 33] is the value of the intracule density $I(\mathbf{u})$ at $\mathbf{u} = 0$, and provides the probability density for an electron pair to collapse at one single point in the \mathbf{r} -space. The electron–electron counterbalance density[34, 35, 36, 37, 38] on the other hand, is the value of $E(\mathbf{R})$ at the origin, $\mathbf{R} = 0$, and gives the probability of finding any two electrons exactly at the opposite (mirror) positions with respect to the origin of coordinates.

3.2. DETERMINATION OF THE ELECTRON COALESCENCE DENSITY THROUGH THE ON-TOP PAIR DENSITY

The electron–electron coalescence density is given by the contraction[32, 33, 39, 40]

$$\begin{aligned} I(0) &= \int \Gamma_2(\mathbf{r}_1, \mathbf{r}_2) \delta(\mathbf{r}_1 - \mathbf{r}_2) d\mathbf{r}_1 d\mathbf{r}_2 \\ &= \frac{1}{2} \int P(\mathbf{r}, \mathbf{r}) d\mathbf{r}, \end{aligned} \tag{50}$$

where the pair distribution function $P(\mathbf{r}, \mathbf{r}) = 2 \int \Gamma_2(\mathbf{r}, \mathbf{r}_2) \delta(\mathbf{r}_2 - \mathbf{r}) d\mathbf{r}_2$ is best known as the *on-top* pair density[41, 42, 43, 44]. The latter expression provides a missing link between these two concepts independently

analyzed in the literature[45, 46, 47]. Notice that it has been found that the electron–electron coalescence density is related to the radiative[48] and relativistic[49] corrections to the atomic energy, and that it can be *measured* experimentally (cf. Sec. 3.3), as shown by Thakkar and Smith in their seminal work on high energy x-ray scattering[50].

In order to analyze the contribution of exchange and correlation effects to the electron–electron coalescence density it is useful to write Eq. (18) for $\mathbf{u} = 0$, namely,

$$I(0) = \frac{1}{2} \int \rho^2(\mathbf{r}) d\mathbf{r} + \frac{1}{2} \int \rho(\mathbf{r}) \rho_{xc}(\mathbf{r}, \mathbf{r}) d\mathbf{r}, \quad (51)$$

where the first integral on the right-hand side is also known as the system averaged electron density[51], $\langle \rho \rangle$. The second term, the on-top exchange–correlation hole density, gives insight into the exchange and correlation between electrons with opposite spins[42, 40]. It has been argued that the correct description of this hole density guarantees the correct performance of density functionals[44]. At the Hartree–Fock level, the departure from the independent particle model is due solely to the exchange correlation. The exchange hole density is known to be:

$$\rho_x(\mathbf{r}, \mathbf{r}) = - \frac{|\rho_\alpha(\mathbf{r}, \mathbf{r})|^2 + |\rho_\beta(\mathbf{r}, \mathbf{r})|^2}{\rho(\mathbf{r})} \quad (52)$$

where the total density $\rho = \rho_\alpha + \rho_\beta$ has been written as the sum of its α and β spin components. Substituting Eq. (52) into Eq. (51) we obtain that,

$$\begin{aligned} I_{\text{HF}}(0) &= \frac{1}{4} \int \rho^2(\mathbf{r}) d\mathbf{r} - \frac{1}{4} \int [\rho_\alpha(\mathbf{r}) - \rho_\beta(\mathbf{r})]^2 d\mathbf{r} \\ &= \int \rho_\alpha(\mathbf{r}) \rho_\beta(\mathbf{r}) d\mathbf{r}, \end{aligned} \quad (53)$$

An alternative derivation of Eq. (53) was given by Ugalde and Sarasola[33]. Lets write Eq. (32) explicitly in terms of the spin orbitals $|m\rangle = \psi_m^{\sigma_m}$, where ψ_m stands for the spatial part and σ_m represents the spin part (either α or β).

$$I_{\text{HF}}(\mathbf{u}) = \frac{1}{2} \sum_{m,n}^N \left(\left[\psi_m^{\sigma_m} \psi_m^{\sigma_m} \mid \hat{\delta} \mid \psi_n^{\sigma_n} \psi_n^{\sigma_n} \right] - \left[\psi_m^{\sigma_m} \psi_n^{\sigma_n} \mid \hat{\delta} \mid \psi_n^{\sigma_n} \psi_m^{\sigma_m} \right] \delta_{\sigma_m, \sigma_n} \right) \quad (54)$$

where $\hat{\delta}$ is a short hand notation for $\delta(\mathbf{u} - \mathbf{r}_1 + \mathbf{r}_2)$ and $\delta_{\sigma_m, \sigma_n}$ is the Kronecker delta. Now, taking into account that

$$\sum_{m,n}^N = \sum_{m=1}^{N^\alpha} \sum_{n=1}^{N^\alpha} + \sum_{m=1}^{N^\alpha} \sum_{n=N^\alpha+1}^N + \sum_{m=N^\alpha+1}^N \sum_{n=1}^{N^\alpha} + \sum_{m=N^\alpha+1}^N \sum_{n=N^\alpha+1}^N \quad (55)$$

where $N = N^\alpha + N^\beta$, being N^α and N^β the number of α and β electrons, respectively. Upon performing the integration over the Dirac's delta, once we have set $\mathbf{u} = 0$, Eq. (54) is readily cast into

$$I_{HF}(0) = \sum_{m=1}^{N^\alpha} \sum_{n=N^\alpha+1}^N \int d\mathbf{r} \psi_m^{\alpha,*}(\mathbf{r}) \psi_m^\alpha(\mathbf{r}) \psi_n^{\beta,*}(\mathbf{r}) \psi_n^\beta(\mathbf{r}) \quad (56)$$

Finally, having in mind that $\rho_\alpha = \sum_{m=1}^{N^\alpha} |\psi_m^\alpha|^2$ and $\rho_\beta = \sum_{m=N^\alpha+1}^N |\psi_m^\beta|^2$, we have proof Eq. (53). Recall that for the restricted closed shell, *i.e.*, the diamagnetic case, $\rho_\alpha = \rho_\beta = \rho/2$, then

$$I_{HF}(0) = \frac{1}{4} \int d\mathbf{r} \rho^2(\mathbf{r}) = \frac{\langle \rho \rangle}{4} \quad (57)$$

This result rationalizes many previous calculations on atomic[35] and molecular[52] systems.

Customarily the exchange-correlation hole is separated into an exchange hole and a correlation hole,

$$\rho_{xc}(\mathbf{r}, \mathbf{r}') = \rho_x(\mathbf{r}, \mathbf{r}') + \rho_c(\mathbf{r}, \mathbf{r}') \quad (58)$$

and the exchange hole is taken equal to the exchange hole of the HF representation (Eq. (52)). In this case, the so represented *exact* electron-electron coalescence density becomes,

$$I(0) = \int \rho_\alpha(\mathbf{r}) \rho_\beta(\mathbf{r}) d\mathbf{r} + \frac{1}{2} \int \rho(\mathbf{r}) \rho_c(\mathbf{r}, \mathbf{r}) d\mathbf{r}, \quad (59)$$

Since the on-top correlation hole $\rho_c(\mathbf{r}, \mathbf{r})$ is either negative or zero[42], Eq. (59) proves that $I(0) < \frac{1}{4} \langle \rho \rangle$. Since the system averaged electron density, $\langle \rho \rangle$, is quantity accessible from experimental data[51], we see that the electron-electron coalescence density constitutes a lower bound to $\langle \rho \rangle$. Explicit calculations for the He isoelectronic series have shown that this bound is tighter than many others found earlier[32]. Recall also that $I(0)$ of Eq. (59) can be estimated by using the wave function methods, then it can be used evaluate the difference between $I(0)$ and $\int \rho_\alpha \rho_\beta d\mathbf{r}$ for large molecules[40], which renders a direct link to the effects of the correlation hole density.

Finally, note in passing that application of the correlation factor definition, Eq. (16), into the intracule density, Eq. (8),

$$I(\mathbf{u}) = \frac{1}{2} \int \rho(\mathbf{r}) \rho(\mathbf{r} + \mathbf{u}) d\mathbf{r} + \frac{1}{2} \int \rho(\mathbf{r}) \rho_{xc}(\mathbf{r}, \mathbf{r} + \mathbf{u}) d\mathbf{r}, \quad (60)$$

provides a useful relation for analyzing the behavior of $I(\mathbf{u})$ with respect to the state represented by the uncorrelated product of densities[53]. The Hartree–Fock J- and K-intracules computed and extensively analyzed by Gill *et al.*[14, 54] constitute a particular realization of this expression when ρ_{xc} is replaced by the exchange hole density, ρ_x .

3.3. EXPERIMENTAL DETERMINATION OF THE ELECTRON COALESCENCE DENSITY THROUGH THE INTEGRATED TOTAL X-RAY SCATTERING INTENSITIES

It is well known that the one- and two-electron properties of atoms and molecules can be inferred from high-energy electron and x-ray scattering experiments[55, 56, 57, 58, 59, 60, 61]. Particularly relevant to this point is the fact that the electron pair distribution is accessible from accurate total x-ray intensities[57, 58, 59, 60, 61]. Theoretical models, on the other hand, clarify the importance of the elastic and inelastic components in describing the electron charge distribution and the role of exchange and correlation effects in the determination of scattered intensities. Thus, it has been concluded that the elastically scattered intensity is sensitive to bond formation in molecules, whereas the inelastic scattering component reflects the electron–electron interaction in the system[60, 61]. Although these studies give insight into the particular electron pair distributions, developments in terms of more simple two-electron functions are desirable. In this section we present a relation between the electron–electron coalescence density and the integrated x-ray scattering intensities. It follows that the former density is an observable that can be used to assess the quality of the theoretical models. In view of the close relationship between the x-ray and high-energy electron scattering in the first Born approximation, this development is also relevant to the theoretical determination of total high-energy electron scattering intensities.

Using the kernel of the Fourier integral transform of the three dimensional Dirac delta function $\delta(\mathbf{r}_1 - \mathbf{r}_2)$,

$$\delta(\mathbf{r}_1 - \mathbf{r}_2) = \left(\frac{1}{2\pi}\right)^3 \int d\boldsymbol{\mu} e^{i\boldsymbol{\mu}\cdot(\mathbf{r}_1 - \mathbf{r}_2)} \quad (61)$$

the electron–electron coalescence density, Eq. (50) is rewritten as

$$\begin{aligned} I(0) &= \left(\frac{1}{2\pi}\right)^3 \int \Gamma_2(\mathbf{r}_1, \mathbf{r}_2) e^{i\boldsymbol{\mu}\cdot(\mathbf{r}_1 - \mathbf{r}_2)} d\mathbf{r}_1 d\mathbf{r}_2 d\boldsymbol{\mu} \\ &= \left(\frac{1}{2\pi}\right)^3 \int G(\boldsymbol{\mu}, -\boldsymbol{\mu}) d\boldsymbol{\mu} \end{aligned} \quad (62)$$

where the structure factor

$$G(\boldsymbol{\mu}, -\boldsymbol{\mu}) = \int \Gamma_2(\mathbf{r}_1, \mathbf{r}_2) e^{i\boldsymbol{\mu} \cdot (\mathbf{r}_1 - \mathbf{r}_2)} d\mathbf{r}_1 d\mathbf{r}_2 \quad (63)$$

represents the transfer of opposite momenta $(\boldsymbol{\mu}, -\boldsymbol{\mu})$ to a pair of electrons located at the same point in the \mathbf{r} -space. The total (\mathcal{I}_t^{xr}) and elastic (\mathcal{I}_{el}^{xr}) x-ray scattered intensities, on the other hand, can be expressed in terms of the density matrices[57]

$$\frac{\mathcal{I}_t^{xr}(\boldsymbol{\mu})}{\mathcal{I}_{cl}} = N + 2 \langle \int \Gamma_2(\mathbf{r}_1, \mathbf{r}_2) e^{i\boldsymbol{\mu} \cdot (\mathbf{r}_1 - \mathbf{r}_2)} d\mathbf{r}_1 d\mathbf{r}_2 \rangle_{\Omega_\mu} \quad (64)$$

and

$$\frac{\mathcal{I}_{el}^{xr}(\boldsymbol{\mu})}{\mathcal{I}_{cl}} = \langle |F(\boldsymbol{\mu})|^2 \rangle_{\Omega_\mu} \quad (65)$$

with

$$F(\boldsymbol{\mu}) = \int \rho(\mathbf{r}) \exp(i\boldsymbol{\mu} \cdot \mathbf{r}) d\mathbf{r} \quad (66)$$

being the so called coherent scattering factor, and $\mathcal{I}_{cl} = (e^2/m_e c)^2$ the classical intensity as given by Thompson[62]. The inelastic x-ray scattering intensity is defined by the difference

$$\frac{\mathcal{I}_{in}^{xr}(\boldsymbol{\mu})}{\mathcal{I}_{cl}} = \frac{1}{\mathcal{I}_{cl}} [\mathcal{I}_t^{xr}(\boldsymbol{\mu}) - \mathcal{I}_{el}^{xr}(\boldsymbol{\mu})] \quad (67)$$

In these equations, the $\langle \dots \rangle_{\Omega_\mu}$ denotes a spherical averaging over the angular part of $\boldsymbol{\mu}$,

$$\langle f(\boldsymbol{\mu}) \rangle_{\Omega_\mu} = \frac{1}{4\pi} \int f(\boldsymbol{\mu}) d\Omega_\mu. \quad (68)$$

Integrating Eq. (64) over the μ variable we obtain

$$\begin{aligned} \frac{1}{\mathcal{I}_{cl}} \int_0^\infty \mathcal{I}_t^{xr}(\mu) \mu^2 d\mu &= N + \frac{2(2\pi)^3}{4\pi} \int \Gamma_2(\mathbf{r}_1, \mathbf{r}_2) \delta(\mathbf{r}_1 - \mathbf{r}_2) d\mathbf{r}_1 d\mathbf{r}_2 \\ &= N + 4\pi^2 I(0) \end{aligned} \quad (69)$$

This equation establishes a link between the electron–electron coalescence density and the experimentally determined total x-ray scattering intensity[63]. The comparison with experimental data, however, is tied to the availability of data for a wide range of incident angles (related to μ) in the experimental measurement of x-ray scattering intensities.

Furthermore, the elastic and inelastic intensities can be related to the charge concentration and the system-averaged on-top exchange-correlation

hole density. To show this, substitute Eq. (51) into Eq. (69) to obtain the integrated total x-ray scattering intensity as

$$\begin{aligned}\mathcal{I}_T &= \frac{1}{\mathcal{I}_{cl}} \int_0^\infty \mathcal{I}_t^{xr}(\mu) \mu^2 d\mu \\ &= N + 2\pi^2 \left\{ \int \rho^2(\mathbf{r}) d\mathbf{r} + \int \rho(\mathbf{r}) \rho_{xc}(\mathbf{r}, \mathbf{r}) d\mathbf{r} \right\}\end{aligned}\quad (70)$$

The integrated form of the elastic x-ray scattering intensity is related to the charge concentration

$$\begin{aligned}\mathcal{I}_e &= \frac{1}{\mathcal{I}_{cl}} \int_0^\infty \mathcal{I}_{el}^{xr}(\mu) \mu^2 d\mu = \int \langle |F(\boldsymbol{\mu})|^2 \rangle_{\Omega_\mu} \mu^2 d\mu \\ &= \int \left\langle \int \rho(\mathbf{r}_1) \rho(\mathbf{r}_2) e^{i\boldsymbol{\mu} \cdot (\mathbf{r}_1 - \mathbf{r}_2)} d\mathbf{r}_1 d\mathbf{r}_2 \right\rangle_{\Omega_\mu} \mu^2 d\mu \\ &= \frac{(2\pi)^3}{4\pi} \int \rho(\mathbf{r}_1) \rho(\mathbf{r}_2) \delta(\mathbf{r}_1 - \mathbf{r}_2) d\mathbf{r}_1 d\mathbf{r}_2 \\ &= 2\pi^2 \int \rho^2(\mathbf{r}) d\mathbf{r}\end{aligned}\quad (71)$$

and finally, the integrated inelastic x-ray scattering intensity, on the other hand, is given by

$$\mathcal{I}_{in} = \frac{1}{\mathcal{I}_{cl}} \int_0^\infty \mathcal{I}_{in}^{xr}(\mu) \mu^2 d\mu = N + 2\pi^2 \int \rho(\mathbf{r}) \rho_{xc}(\mathbf{r}, \mathbf{r}) d\mathbf{r}\quad (72)$$

Recall that our Eq. (71) generalizes a previous result by Hyman *et al.*[51] for a sample of N identical non-overlapping atoms of finite size. The above integrated formulae corroborate the theoretical interpretation attributed to these components: the elastic component is related to the electron distribution and inelastic component is mostly concerned with the details of electron-electron interactions.

Eq. (70-72) constitute one strong bridge between experiment and theory. On the one hand experimental work can provide values for the scattering intensities \mathcal{I}_t^{xr} and \mathcal{I}_{el}^{xr} and on the other hand theoreticians can obtain accurate system average electron densities $\langle \rho \rangle$, and design reliable exchange-correlation hole density functions, $\rho_{xc}(\mathbf{r}, \mathbf{r}')$. These two independent developments must fulfill the requirements imposed by Eq. (70-72). In particular, it would be highly desirable that approximate density functionals should reproduce the experimentally obtained integrated intensities of Eq. (70-72), in view of the importance of $\rho_{xc}(\mathbf{r}, \mathbf{r}')$ in modeling the correct electron pair distribution[44].

4. Properties of the Extracule Density

As stated above the topology of the extracule density, $E(\mathbf{R})$, is substantially more involved than that of the more familiar electron density $\rho(\mathbf{r})$. However, following earlier work[25, 64] on simple diatomic molecules, Duran *et al.*[53, 65, 66, 67] have expanded the study of $E(\mathbf{R})$ to more complex molecules. Although much work remains to be carried out, encouraging preliminary results have been reported by the Girona group in terms of their *Valence Bond* interpretation of the extracule density[68].

We have shown in the preceding section (cf. Sec. 3.2) that one useful step towards a simplified description of the electron pairs densities consists of looking at their values at the origin. Thus, for example, we have been able to link (see Eq. 72) the *inelastic* x-ray scattering intensity with the system averaged exchange-correlation hole density.

The value of $E(\mathbf{R})$ at $\mathbf{R} = 0$, known as the electron-electron counterbalance density, has been also studied earlier[34, 35, 36, 38, 69, 70, 71] and, we will review some of its salient properties below.

4.1. THE ELECTRON COUNTERBALANCE DENSITY AND ELECTRON CORRELATION EFFECTS IN ATOMS.

Let's consider atoms first. Koga and Matsuyama[34, 35] have calculated the electron–electron counterbalance density for the first 92 atoms and their respective cations at the Hartree-Fock level of theory. Now, what would be the effect of the post Hartree-Fock electron correlation on the electron counterbalance density ?. One can foresee two different scenarios, namely:

- If the Post-HF electron counterbalance density is larger than the electron counterbalance density at the HF level of theory, clearly this is because the effect of the electron correlation is to increase the probability to find the electrons of the electron pair, on opposite sides of the nucleus. Namely, there is an increase of the so-called *non-dynamical* or *angular* correlation (see Table 1 and its subsequent discussion).
- If the Post-HF electron counterbalance density is smaller than the electron counterbalance density at the HF level of theory, the effect of the electron correlation is to increase the probability of finding the electrons of the electron pair on the same side with respect to the nucleus. Namely, electron correlation is mainly of *radial* type (see Table 1 and its subsequent discussion).

Explicit post-HF calculations of the electron counterbalance density for the atoms of the first row of the periodic table from Li to Ne, have revealed that the *radial* correlation dominates over the *angular* correlation all along the row[38]. Namely, the post-HF electron counterbalance density is smaller than the HF electron counterbalance density. However, as shown in Table

3 there are a few other subtleties of the electron correlation that are worth

TABLE 3. The electron-electron counterbalance density for the ground state of selected atoms of the first row calculated at three different levels of theory

	Li	Be	B	C
HF	6.272706	16.79124	35.50149	65.49247
FCI	5.753893	15.85480	33.98779	63.24212
MCSCF	6.273351	16.82768	35.56544	65.59269

to point them out. Thus, first of all, comparison of the HF entries with the FCI entries confirms that the electron–electron counterbalance density decreases as a consequence of including electron correlation effects. Hence, for atoms, the HF method lacks *mainly* for a proper accounting of the *radial* correlation, which is essentially *dynamic* electron correlation.

On the other hand comparison of the MCSCF entries with both HF and FCI entries of Table 3, reveals that the *MultiConfigurational Self Consistent Field* (MCSCF) method overweights the *non-dynamical*, or *angular* electron correlation with respect to the *dynamical*, or *radial* electron correlation. Notice, that the MCSCF increases the electron-electron counterbalance density with respect to the HF, opposite to the behavior found for the FCI method. These findings are consistent with the warnings raised by Borden and Davidson[72] on the failures due the unbalance between the *dynamical* and *non-dynamical* electron correlation effects induced by not including enough electrons in the MCSCF *active space*.

The above discussion has made it clear that both the *dynamical* and the *non-dynamical* correlation effects can be displayed through the direct evaluation of the electron counterbalance density, the reason being that the spatial electron separation introduced by correlating orbitals of different angular symmetry can be readily traced by the $E(0)$ values.

In particular, it follows that *angular* electron correlation, represented by high angular momentum correlating orbitals, which have only one node at the nucleus, has a *non-dynamical* character. Whereas, *radial* electron correlation exhibits mainly *dynamical* character and it is associated with orbitals contributing to more than one atomic shell and having several nodes in their radial part. Thus, a maximum $E(0)$ values can be used a criterion to select a wave function that would include the maximum *non-dynamical* electron correlation of the system.

This hypothesis has been checked[71] by explicit calculations on the beryllium-atom isoelectronic series, which constitutes an ideal target be-

cause the presence of the $2s^2 - 2p^2$ pseudo-degeneracy gives rise to an appreciable *non-dynamical* component[73]. It is expected that a first-order approximation should involve only these two configurations. However, since the active space is much larger, a nontrivial set of virtual orbitals must be analyzed to clarify the effects of extending the active space on the non-dynamical correlation energy component.

The (dynamical) Coulomb hole was first alluded to by Debye[74] in 1925 and then calculated, for the first time, for the ground state of the He atom by Coulson and Neilson[75] in 1961. Since then a wealth of information about the Coulomb hole has been produced[10]. The usual definition of the Coulomb hole is the difference between the *exact* and the HF radial intracule densities

$$\Delta I_{Coul}(u) = 4\pi u^2 [h_{exact}(u) - h_{HF}(u)]. \quad (73)$$

This difference is customarily ascribed to the improper handling of the electron-electron interactions within the HF scheme, in a dynamical sense. However, as we have seen in the previous section, electron correlation also includes a system-dependent part. This part, namely, the non-dynamical correlation, has been neglected as such in all the calculations reported so far on the Coulomb hole, moreover it has been usually mixed with the system independent, *universal*, part, namely, with the dynamical correlation.

Clearly, in order to learn more about the two parts of the electron correlation separately, we have to be able to separate them. We have argued in the previous section that a criterion to carry out this separation consists of maximizing the counterbalance density. The so obtained wave function will, therefore, account for all the *non-dynamical* portion. The remaining piece will be the dynamical electron correlation. Notice that this partition scheme leads us to consider two holes, the non-dynamical Coulomb hole and the dynamical Coulomb hole. Thus, the non-dynamical correlation hole is defined by the difference between the correlated $h_c(u)$ and the Hartree-Fock $h_{HF}(u)$ radial densities

$$\Delta I_{nd}(u) = 4\pi u^2 [h_c(u) - h_{HF}(u)] \quad (74)$$

In this way, the non-dynamical Coulomb hole for the Be sequence is obtained by subtracting the radial intracule densities calculated from the wave functions $1s^2\{2s,2p,3p\}^2$ and HF.

We have evaluated this quantity for the isoelectronic series of the Be atom and the resulting plots are shown in Fig. 6. A scaling factor of $Z_{eff} = Z - 2$ has been used in order to embody the screened effective charge seen by the valence electrons. Benesh and Smith[76] pointed out earlier that the non-dynamical hole for the Be isoelectronic series must be

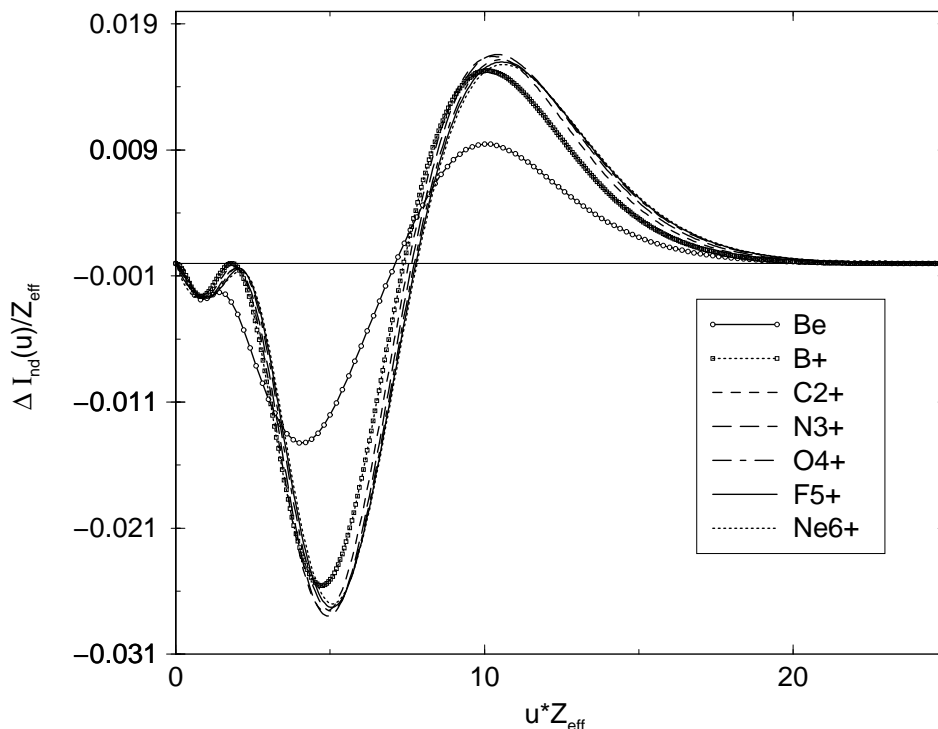


Figure 6. The scaled non-dynamical Coulomb hole $\Delta I_{nd}(u)$ as a function of the interelectronic distance, u , for the Be isoelectronic series (scaling factor is $Z_{eff} = Z - 2$).

localized primarily in the L shell for it accounts solely for the $2s - 2p$ near-degeneracy effect and indeed they calculated this non-dynamical hole using a frozen-core CI wave function of Watson[77]. Our non-dynamical hole and theirs are very similar. This gives additional support to our electron correlation separation criteria. Also, from Fig. 6 it can be observed that this system-specific portion of the electron correlation has a very simple shape, *e.g.* it is negative at short interelectronic distances and positive for larger interelectronic distances. The shoulder on the non-dynamical Coulomb hole at short interelectronic distances, simply reflects the fact that the orbitals from the HF determinant in $1s^2\{2s,2p,3p\}^2$ have changed during the MC-SCF procedure with respect to the initial HF orbitals, as expected. At large interelectronic distances, a Z converged pattern appears showing that at large Z the non-dynamical hole retains a unique character and remains constant.

Recently, Gálvez *et al.*[78] have reported the total Coulomb hole for the isoelectronic series of beryllium as calculated from a HF wave function and from a correlated Monte Carlo type wave function. Their resulting total

Coulomb hole has a remarkable resemblance to our *non-dynamical* hole. This indicates that correlated Monte Carlo wave functions constructed from a minimal MCSCF kernel and a correlation factor do not account for too much of the dynamical electron correlation effects. Further support for this point comes from the comparison of the electron-electron counterbalance density values calculated from correlated Monte Carlo wave functions with the values calculated from MCSCF wave functions having only the valence electrons in the active space (see Table 3).

The dynamical Coulomb hole is defined by the difference between the exact (FCI) $h_{FCI}(u)$ and the correlated $h_c(u)$ radial intracule densities

$$\Delta I_d(u) = 4\pi u^2 [h_{FCI}(u) - h_c(u)] \quad (75)$$

The dynamical Coulomb hole for the Be isoelectronic series has been calculated as the intracule density obtained from the full CI wave function minus that obtained from the wave function $1s^2\{2s,2p,3p\}^2$. Contrary to the non-dynamical, the dynamical Coulomb hole shows a rather complex structure, as seen from the inspection of Figure 7. The complex oscillatory structure of the dynamical Coulomb hole for the Be sequence can be rationalized by invoking the K-L inter-shell correlation, which is usually hidden by the much larger non-dynamical contribution of the total Coulomb hole. Indeed, Banyard and Mobbs[79] demonstrated that this oscillatory behavior of the Coulomb hole arises when it is evaluated from the pair-correlation function of explicitly correlated wave functions. Clearly, since the pair-correlation function accounts for the dynamical electron correlation the present calculations are supportive of our criterion of maximum electron-electron counterbalance density as utilized to separate non-dynamical and dynamical parts of the electron correlation.

In general, it can be concluded that angular correlation, represented by high angular momentum correlating orbitals, has a long-range (non-dynamical) character whereas radial correlation exhibits a short range (dynamical) nature due to its low angular momentum and intrashell orbitals. Thus, a maximum $E(0)$ value can be used as a criterion to select a wave function that would include the maximum non-dynamical correlation. This idea has been placed in its proper context by Cremer in a recent enlightening review[80]

4.2. THE ELECTRON COUNTERBALANCE DENSITY AND ELECTRON CORRELATION EFFECTS IN MOLECULES.

The criterion of maximum electron counterbalance density can also be used to understand the non-dynamical correlation effects arising from the dissociation process of the H_2 molecule. In the region close to the equilibrium

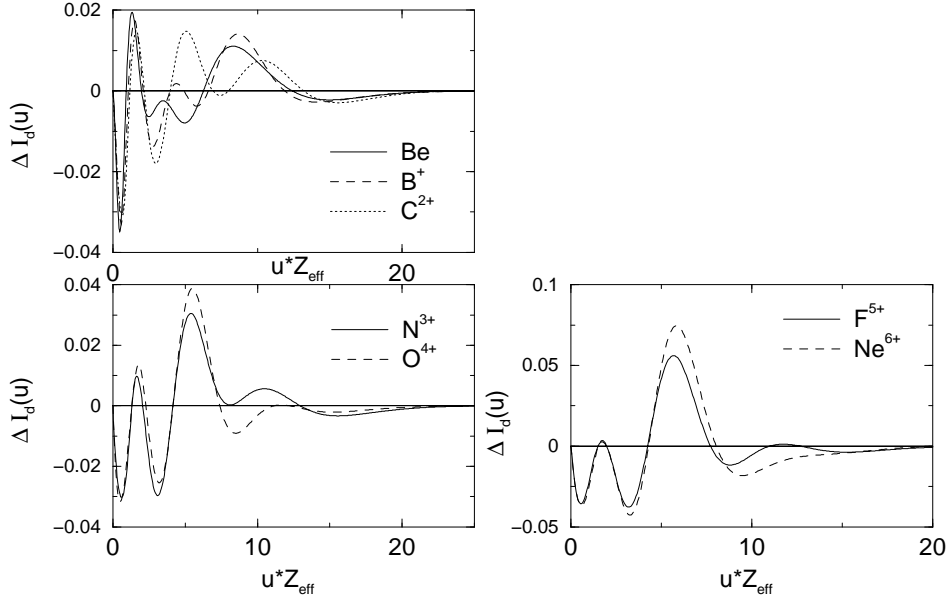


Figure 7. The scaled dynamical Coulomb hole $\Delta I_d(u)$ as a function of the interelectronic distance, u , for the Be isoelectronic series (scaling factor is $Z_{eff} = Z - 2$).

distance, this system can be regarded as *normal*, *i.e.* non-dynamical effects are negligible. Recall that for $R=1.4$ a.u, the coefficient of the CI wave function was $c=-0.1134$ (see Eq. 7). As the bond is stretched, proper dissociation must be described with a configuration interaction wave function that includes the rising *non-dynamical* effects and shifts value of coefficient $c=1$ (see Eq. 5). Thus, it is expected that the electron counterbalance density should be very sensitive to the molecular dissociation.

Figure 8 shows the changes in the electron-electron coalescence density, $E(0)$, during the dissociation of the H_2 molecule. Three different levels of theory are used in this calculation. The correct general behavior is already displayed by the 2-CSF wave function, which reproduces the exact value of $E(0)$ for $R \rightarrow \infty$. Namely, the exact dissociated wave function for H_2 is Eq. (1) and, consequently the electron counterbalance density is

$$\begin{aligned}
 E(0) &= \int |\Psi(\mathbf{r}_1, \mathbf{r}_2)|^2 \delta\left(\frac{\mathbf{r}_1 + \mathbf{r}_2}{2}\right) d\mathbf{r}_1 d\mathbf{r}_2 \\
 &= 2^3 \frac{1}{2} \left[2 \int \psi_A^2(1) \psi_B^2(2) \delta(\mathbf{r}_1 + \mathbf{r}_2) d\mathbf{r}_1 d\mathbf{r}_2 \right. \\
 &\quad \left. + 2 \int \psi_A(1) \psi_B(2) \psi_A(2) \psi_B(1) \delta(\mathbf{r}_1 + \mathbf{r}_2) d\mathbf{r}_1 d\mathbf{r}_2 \right]
 \end{aligned}$$

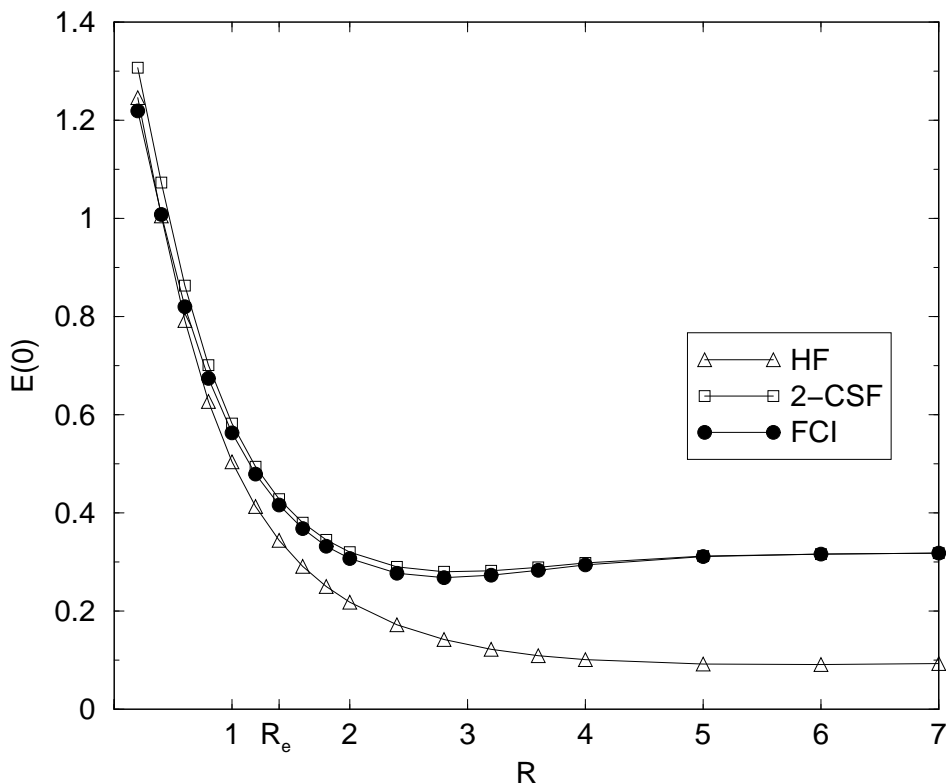


Figure 8. The electron counterbalance density, $E(0)$, as a function of the internuclear distance R , in a.u., for H_2 . The equilibrium bond distance, R_e , is labeled on the R -axis

$$\begin{aligned}
&= 2^3 \left[\int \psi_A^2(\mathbf{r}_1) \psi_B^2(-\mathbf{r}_1) d\mathbf{r}_1 \right. \\
&\quad \left. + \int \psi_A(\mathbf{r}_1) \psi_B(-\mathbf{r}_1) \psi_A(-\mathbf{r}_1) \psi_B(\mathbf{r}_1) d\mathbf{r}_1 \right] \quad (76)
\end{aligned}$$

and bearing in mind that $\psi_{A,B}(\mathbf{r}) = \exp(-|\mathbf{r}_1 \pm \mathbf{R}/2|) / \sqrt{\pi}$, it is obtained that

$$\begin{aligned}
\int \psi_A^2(\mathbf{r}_1) \psi_B^2(-\mathbf{r}_1) d\mathbf{r}_1 &= \frac{1}{\pi^2} \int d\mathbf{r}_1 e^{-4|\mathbf{r}_1 + \mathbf{R}/2|} \\
&= \frac{1}{\pi^2} 2\pi \int_0^\infty r_1^2 \int_{-1}^1 d\mu e^{-4\sqrt{r_1^2 + R^2/4 + r_1 R \mu}} \\
&= \frac{1}{2^3 \pi} \quad (77)
\end{aligned}$$

after a little algebra. Analogously, the second integral of the right hand side

of Eq. (76) can be cast into

$$\frac{1}{\pi^2} \int d\mathbf{r}_1 e^{-2|\mathbf{r}_1+\mathbf{R}/2|-2|\mathbf{r}_1-\mathbf{R}/2|} = \int d\mathbf{r}_1 \psi_A^2(\mathbf{r}_1) \psi_B^2(\mathbf{r}_1) = 0 \quad (78)$$

Hence, substituting Eq.'s (77,78) into Eq. (76) we finally obtain that for stretched H_2 , the electron counterbalance density is,

$$E(0) = \frac{1}{\pi} \quad (79)$$

Closer inspection of Figure 8 reveals that it is not only the correct behavior of $E(0)$ at large internuclear separation R what is granted, but also the appearance of a *relevant* feature of $E(R)$, which is not present at the HF level of theory, is due to the role played by the second determinant of the Eq. (4). Recall that this determinant constitutes the only extra configuration apart from the reference HF one, contributing to the 2-CSF wave function. We would like, at this point, to draw attention to the minimum shown by the correlated $E(0)$ functions in Figure 8.

The location of this minimum at $R_o = 2.8$, does not coincide with the equilibrium distance, R_e . In this case, however, this minimum can be related to the minima found for quantities that depend on the momentum operator, $\hat{\mathbf{p}}$. In fact, the more rapidly the electrons move through the molecular space, the higher the probability of finding two electrons at opposite points with respect to the origin of coordinates. This relationship can be readily explained by writing $E(0)$ in terms of the kernel of the Fourier transformations (FT) for the Dirac delta function, $\delta(\mathbf{r}_1 + \mathbf{r}_2) = (2\pi)^{-3} \int \exp[-i\boldsymbol{\mu} \cdot (\mathbf{r}_1 + \mathbf{r}_2)] d\boldsymbol{\mu}$, thus,

$$\begin{aligned} E(0) &= 8 \int \Gamma_2(\mathbf{r}_1, \mathbf{r}_2) \delta(\mathbf{r}_1 + \mathbf{r}_2) d\mathbf{r}_1 d\mathbf{r}_2, \\ &= 8 (2\pi)^{-3} \int \Gamma_2(\mathbf{r}_1, \mathbf{r}_2) e^{-i\boldsymbol{\mu} \cdot (\mathbf{r}_1 + \mathbf{r}_2)} d\boldsymbol{\mu} d\mathbf{r}_1 d\mathbf{r}_2, \\ &= 8 \int F_2(\boldsymbol{\mu}, \boldsymbol{\mu}) d\boldsymbol{\mu} \end{aligned} \quad (80)$$

with the second-order form factor[81]

$$F_2(\boldsymbol{\mu}, \boldsymbol{\mu}) = (2\pi)^{-3} \int \Gamma_2(\mathbf{r}_1, \mathbf{r}_2) e^{-i\boldsymbol{\mu} \cdot (\mathbf{r}_1 + \mathbf{r}_2)} d\mathbf{r}_1 d\mathbf{r}_2, \quad (81)$$

given by the FT of the diagonal of the second-order density matrix. Notice, however, that here the minus sign is chosen in the exponential as opposed to the plus sign usually employed. Since

$$F_2(\boldsymbol{\mu}, \boldsymbol{\mu}) = \int \Pi(\mathbf{p}_1 + \boldsymbol{\mu}, \mathbf{p}_2 + \boldsymbol{\mu}; \mathbf{p}_1, \mathbf{p}_2) d\mathbf{p}_1 d\mathbf{p}_2 \quad (82)$$

with $\Pi(\mathbf{p}_1, \mathbf{p}_2; \mathbf{p}'_1, \mathbf{p}'_2)$ being the second-order density matrix in \mathbf{p} -space,

$$\begin{aligned} \Pi(\mathbf{p}_1, \mathbf{p}_2; \mathbf{p}'_1, \mathbf{p}'_2) &= (2\pi)^{-6} \int d\mathbf{r}_1 d\mathbf{r}_2 d\mathbf{r}'_1 d\mathbf{r}'_2 \Gamma_2(\mathbf{r}_1, \mathbf{r}_2; \mathbf{r}'_1, \mathbf{r}'_2) \\ &\times e^{-i(\mathbf{r}_1 \cdot \mathbf{p}_1 - \mathbf{r}'_1 \cdot \mathbf{p}'_1) - i(\mathbf{r}_2 \cdot \mathbf{p}_2 - \mathbf{r}'_2 \cdot \mathbf{p}'_2)}, \end{aligned} \quad (83)$$

the electron-electron counterbalance density, $E(0)$, is obtained from the second-order momentum density matrix disturbed by an equal amount of momentum transfer, $\boldsymbol{\mu}$. This relation can be used to explain the coincidence between the minimum attained by the changes in the kinetic energy, $\Delta T(R)$, calculated as the difference between the molecular value at a given separation R and the value at infinite separation[82], and the minimum shown in $E(0)$. This minimum is congruent with the increasing accumulation of density between the approaching nuclei, thereby accounting for an initial decrease in $\Delta T(R)$ and $E(0)$. At the point R_o , the increasing density transfer leads to a contraction of the density towards the bonding region and $\Delta T(R)$ and $E(0)$ begin a steep increase in attaining the values characteristic of equilibrium. Finally, at short internuclear distances the charge accumulation in the bonding region leads to an abrupt increase in both the kinetic energy and $E(0)$ values.

The changes in the electron density in the interaction between a pair of H atoms can also be examined by resorting to the atomic Ehrenfest force.[82, 83] This force is defined as the force exerted on an open system Ω by the electron density at \mathbf{r} , averaged over the motions of the remaining electrons,

$$F(\Omega) = \int_{\Omega} \mathbf{F}(\mathbf{r}) d\mathbf{r} \quad (84)$$

where $\mathbf{F}(\mathbf{r}) = \int d\tau' \Psi^*(-\nabla_{\mathbf{r}} V)\Psi$ is the force density and V the total potential operator with its gradient given by the commutator $(i/\hbar)[\hat{H}, \hat{\mathbf{p}}] = -\nabla_{\mathbf{r}} V$. The mode of integration $\int d\tau'$ assumes a summation over all spins and an integration over all space coordinates, except \mathbf{r} , the coordinate of the open system. The force density $\mathbf{F}(\mathbf{r})$ attains a maximum value at the point R_o where $-\nabla_{\mathbf{r}} V$ in turn has a maximum. Since the latter force is the force exerted on an electron at \mathbf{r} by the remaining electrons and nuclei located in a fixed position, it is expected that the maximum force corresponds to the situation where electrons have the lower kinetic energy, or equivalently, where $E(0)$ hits a minimum value. Thus, at R_o , the electrostatic force of attraction exerted on the electron density in the atomic basin by the nuclei and the repulsive force exerted by all remaining electrons attain a maximum coincident with the minimum in $E(0)$.

5. Acknowledgment

This research has been funded by Euskal Herriko Unibertsitatea (the University of the Basque Country), Eusko Jaurlaritza (the Basque Government) and the Spanish Ministry of Science and Technology. JMU wishes to thank Prof. Russell J. Boyd for much encouragement and dedicated guidance over the years across the exciting field of electron pair densities.

References

1. Heitler, W.; London, F. *Z. Phys.* **1927**, *44*, 455.
2. Hartree, D. R. *Proc. Cambridge Philos. Soc.* **1928**, *24*, 89.
3. Fock, V. *Z. Phys.* **1930**, *61*, 126.
4. Slater, J. C. *Phys. Rev.* **1930**, *35*, 210.
5. Helgaker, T.; Jorgensen, P.; Olsen, J. *Molecular Electronic Structure Theory*; John Wiley & Sons Ltd.: West Sussex, England, 2000.
6. Kolos, W.; Wolniewicz, L. *J. Chem. Phys.* **1968**, *49*, 404.
7. Heinemann, H. D.; Kolb, D.; Fricke, B. *Chem. Phys. Lett.* **1987**, *137*, 180.
8. Handy, N. C.; Cohen, A. J. *Mol. Phys.* **2001**, *99*, 403.
9. Cohen, A. J.; Handy, N. C. *Mol. Phys.* **2001**, *99*, 607.
10. Valderrama, E.; Ugalde, J. M.; Boyd, R. J. In *Many-Electron Densities and Reduced Density Matrices*; Cioslowski, J., Ed.; Kluwer Academic/Plenum Publishers: New York, 2000; pages 231–248.
11. McWeeny, R. *Rev. Mod. Phys.* **1960**, *32*, 335.
12. Hohenberg, P.; Kohn, W. *Phys. Rev.* **1964**, *140*, A1133.
13. Maitra, N. T.; Burke, K. In *Many-Electron Densities and Reduced Density Matrices*; Cioslowski, J., Ed.; Kluwer Academic/Plenum Publishers: New York, 2000; pages 183–208.
14. Lee, A. M.; Gill, P. M. W. *Chem. Phys. Letters* **1999**, *313*, 271.
15. Cioslowski, J.; Liu, G. *J. Chem. Phys.* **1998**, *109*, 8225.
16. Bartlett, R. J.; Stanton, J. F. In *Reviews in Computational Chemistry*; Lipkowitz, K. B., Boyd, D. B., Eds.; VCH: New York, 1994; pages 65–169.
17. Szabó, A.; Ostlund, N. S. *Modern Quantum Chemistry*; McGraw-Hill: New York, 1989.
18. Boyd, R. J.; Sarasola, C.; Ugalde, J. M. *J. Phys. B* **1988**, *21*, 2555.
19. Tal, Y.; Katriel, J. *J. Phys. B* **1974**, *16*, 2113.
20. Rothenberg, S.; Davidson, E. D. *J. Chem. Phys.* **1966**, *45*, 2560.
21. Katriel, J. *Phys. Rev. A* **1972**, *5*, 1990.
22. Katriel, J.; Pauncz, R. *Adv. Quantum Chem.* **1977**, *10*, 143.
23. Ugalde, J. M.; Boyd, R. J. *Chem. Phys. Lett.* **1985**, *114*, 197.
24. Darvesh, K. V.; Boyd, R. J. *J. Chem. Phys.* **1987**, *87*, 5329.
25. Thakkar, A. J.; Moore, N. J. *Int. J. Quantum Chem., Quantum Chem. Symp.* **1981**, *15*, 393.
26. Thakkar, A. J.; Tripathi, A. N.; Smith, Jr, V. H. *Int. J. Quantum Chem.* **1984**, *26*, 157.
27. Cioslowski, J.; Liu, G. *J. Chem. Phys.* **1996**, *105*, 8187.
28. Fradera, X.; Duran, M.; Mestres, J. *J. Chem. Phys.* **1997**, *107*, 3576.
29. Fradera, X.; Sarasola, C.; Ugalde, J. M.; Boyd, R. J. *Chem. Phys. Letters* **1999**, *304*, 393.
30. Cioslowski, J.; Liu, G. *J. Chem. Phys.* **1999**, *110*, 1882.
31. Cioslowski, J.; Liu, G.; Rychlewski, J.; Cancek, W.; Komasa, J. *J. Chem. Phys.* **1999**, *111*, 3401.
32. Dehesa, J. S.; Angulo, J. C.; Koga, T.; Matsui, K. *Phys. Rev. A* **1993**, *47*(6), 5202.

33. Ugalde, J. M.; Sarasola, C. *Phys. Rev. A* **1994**, *49*, 3081.
34. Koga, T.; Matsuyama, H. *J. Phys. B* **1997**, *30*, 5631–5641.
35. Koga, T.; Matsuyama, H. *J. Chem. Phys.* **1997**, *107*, 10062.
36. Koga, T. *J. Chem. Phys.* **1998**, *108*, 2515.
37. Gálvez, F. J.; Buendía, E.; Sarsa, A. *J. Chem. Phys.* **1999**, *111*(8), 3319.
38. Mercero, J. M.; Fowler, J. E.; Sarasola, C.; Ugalde, J. M. *Phys. Rev. A* **1999**, *59*, 4255.
39. Matsuyama, H.; Koga, T.; Romera, E.; Dehesa, J. S. *Phys. Rev. A* **1998**, *57*(3), 1759.
40. Fradera, X.; Duran, M.; Valderrama, E.; Ugalde, J. M. *Phys. Rev. A* **2000**, *62*, 34502.
41. Becke, A.; Savin, A.; Stoll, H. *Mol. Phys.* **1995**, *91*, 147.
42. Perdew, J. P.; Savin, A.; Burke, K. *Phys. Rev. A* **1995**, *51*, 4531–4541.
43. Perdew, J. P.; Ernzerhof, M.; Burke, K.; Savin, A. *Int. J. Quantum Chem.* **1997**, *61*, 197.
44. Burke, K.; Perdew, J. P.; Ernzerhof, M. *J. Chem. Phys.* **1998**, *109*, 3760.
45. Valderrama, E.; Ugalde, J. M. in: *DFT-2000, Satellite Symposium of the 10th International Congress of Quantum Chemistry, Menton, France, Abstract P72, 11-14 2000*.
46. Valderrama, E.; Ugalde, J. M. *Int. J. Quantum Chem.* **2002**, *86*, 40.
47. Koga, T. *J. Chem. Phys.* **2001**, *114*, 102.
48. Kabir, P. K.; Salpeter, E. *Phys. Rev.* **1957**, *108*, 1256.
49. Bethe, H. A.; Salpeter, E. *Quantum Mechanics of One- and Two- Electron Atoms*; Plenum: New York, 1977.
50. Thakkar, A. J.; Smith, Jr., V. H. *J. Phys. B* **1978**, *11*, 3803.
51. Hyman, A. S.; Yaniger, S. I.; Liebman, J. F. *Int. J. Quantum Chem.* **1978**, *14*, 757.
52. Solà, M.; Mestres, J.; Oliva, J. M.; Duran, M.; Carbó, R. *Int. J. Quantum Chem.* **1996**, *58*(4), 361.
53. Fradera, X.; Duran, M.; Mestres, J. *J. Chem. Phys.* **2000**, *113*, 2530.
54. Gill, P. M. W.; Lee, A. M.; Nair, N.; Adamson, R. D. *J. Mol. Struct. (THEOCHEM)* **2000**, *506*, 303.
55. Kohl, D. A.; Bartell, L. S. *J. Chem. Phys.* **1969**, *51*, 2891.
56. Kohl, D. A.; Bartell, L. S. *J. Chem. Phys.* **1969**, *51*, 2896.
57. Benesh, R.; Smith, Jr., V. H. *Acta Cryst.* **1970**, *A 26*, 579.
58. Stewart, R. F. *Isr. J. of Chem.* **1977**, *16*, 116.
59. Boyd, R. J.; Ugalde, J. M. In *Computational Chemistry, Part A*; Fraga, S., Ed.; Elsevier: Amsterdam, 1992; pages 273–299.
60. Wang, J.; Tripathi, A. N.; Smith, Jr, V. H. *J. Chem. Phys.* **1994**, *101*(6), 4842.
61. Watanabe, N.; Hayashi, H.; Udagawa, Y.; Ten-no, S.; Iwata, S. *J. Chem. Phys.* **1998**, *108*(11), 4545.
62. Thompson, J. J.; Thompson, G. P. *Conduction of Electricity through Gases*, Vol. II; Cambridge Univ. Press: Cambridge, 3rd. ed., 1933.
63. Valderrama, E.; Fradera, X.; Ugalde, J. M. *Phys. Rev. A* **2001**, *64*, 044501.
64. Sarasola, C.; Ugalde, J. M.; Boyd, R. J. *J. Phys. B.* **1990**, *23*, 1095.
65. Fradera, X.; Duran, M.; Mestres, J. *Can. J. Chem.* **2000**, *78*, 328.
66. Fradera, X.; Duran, M.; Mestres, J. *J. Phys. Chem. A* **2000**, *104*, 8445.
67. Fradera, X.; Duran, M.; Mestres, J. *J. Comp. Chem.* **2000**, *21*, 1361.
68. Poater, J.; Sola, M.; Duran, M.; Fradera, X. *J. Phys. Chem. A* **2001**, *105*, 2052.
69. Koga, T.; Matsuyama, H. *Int. J. Quantum Chem.* **1999**, *74*, 455.
70. Valderrama, E.; Fradera, X.; Ugalde, J. M. *J. Chem. Phys.* **2001**, *115*, 1987.
71. Valderrama, E.; Mercero, J. M.; Ugalde, J. M. *J. Phys. B* **2001**, *34*, 275.
72. Borden, W. T.; Davidson, E. R. *Acc. Chem. Res* **1996**, *29*(2), 67.
73. Valderrama, E.; Ludeña, E. V.; Hinze, J. *J. Chem. Phys.* **1999**, *110*, 2343.
74. Debye, P. *J. Math. Phys.* **1925**, *4*, 133.
75. Coulson, C. A.; Neilson, A. H. *Proc. Phys. Soc.* **1961**, *78*, 831.

76. Benesh, R.; Smith, Jr., V. H. *J. Chem. Phys.* **1971**, *55*, 482.
77. Watson, R. *Ann. Phys. (NY)* **1961**, *13*, 250.
78. Gálvez, F. J.; Buendía, E.; Sarsa, A. *J. Chem. Phys.* **1999**, *111*(24), 10903.
79. Banyard, K. E.; Mobbs, R. J. *J. Chem. Phys.* **1981**, *75*, 3432.
80. Cremer, D. *Mol. Phys.* **2001**, *99*, 1899.
81. Thakkar, A. J.; Simas, A. M.; Smith, Jr., V. H. *Chem. Phys.* **1981**, *63*, 175.
82. Hernández-Trujillo, J.; Bader, R. F. W. *J. Phys. Chem. A* **2000**, *104*, 1779.
83. Bader, R. F. W. *J. Phys. Chem. A* **1998**, *102*, 7314.